recent study showing that intensive IVIR was an independent factor associated with a decreased survival and higher rates of hospitalization for HD patients [39]. HD patients have relatively lower serum albumin levels for several reasons, including malnutrition. Given the fact that albumin is a major antioxidant in the extracellular fluid, a decrease in serum albumin levels in these patients would contribute to the high incidence of cardiovascular events that are frequently associated with an increase in oxidative stress. Significance of oxidized serum albumin in HD patients in the progression of cardiovascular diseases is not fully determined. However, in the case of HD patients, it has been demonstrated that the carotid artery intima-media thickness is associated with the level of plasma advanced oxidation protein products (AOPP), serum ferritin, and the annual intravenous iron dose administered [40], and that AOPP is mostly due to albumin [41]. These findings suggest the possibility that oxidized albumin in HD patients might play a pathogenic role in the progression of atherosclerosis. A study by Boaz et al has suggested that antioxidant therapy may lessen cardiovascular complications in end-stage renal disease patients [42], suggesting the importance of evaluating oxidative stress and the appropriate antioxidant therapy in HD patients, especially in patients who are receiving IVIR. The coadministration of antioxidants such as vitamin E with IVIR has been shown to be effective in reducing oxidative stress in HD patients [43]. HPLC analysis of serum albumin represents a potentially useful marker for the qualitative and quantitative evaluation of oxidative stress in HD patients, as well as for the assessment of the effect of antioxidant therapy.

CONCLUSION

The findings here suggest that IVIR is associated with an increase in the oxidative state of serum albumin, and that the HPLC analysis of serum albumin would be a useful marker for the quantitative and qualitative evaluation of oxidative stress in HD patients.

ACKNOWLEDGMENT

The authors thank Drs. Ken Imanishi, Kenji Machida, Shiho Wakamatsu, Saeko Tajiri (Department of Nephrology, Kumamoto University Graduate School of Medical Sciences, Kumamoto, Japan), and Dr. Motoko Tanaka (Department of Nephrology, Akebono Clinic, Kumamoto, Japan) for blood sample collection from HD patients and for helpful discussions. This work was supported by the Grants-in-Aid for Scientific Research from the Ministry of Education, Culture, Sports, Science and Technology in Japan (13770602 and 15790432 to K.K., 14370759 and 14657618 to M.O., 13877166 and 14370321 to K.T.), and the Salt Science Research Foundation (to K.K.).

Reprint requests to Kenichiro Kitamura, M.D., Ph.D., Assistant Professor, Department of Nephrology, Kumamoto University Graduate School of Medical Sciences, 1-1-1 Honjo, Kumamoto, Kumamoto 860-8556, Japan.
E-mail: ken@gpo.kumamoto-u.ac.jp

REFERENCES

1. Descamps-Latscha B, Witko-Sarsat V: Importance of oxidatively modified proteins in chronic renal failure. *Kidney Int* (Suppl 78):S108–S113, 2001
2. Daschner M, Lenhartz H, Botticher D, *et al*: Influence of dialysis on plasma lipid peroxidation products and antioxidant levels. *Kidney Int* 50:1268–1272, 1996
3. Himmelfarb J, McMonagle E: Albumin is the major plasma protein target of oxidant stress in uremia. *Kidney Int* 60:358–363, 2001
4. Lee Y, Shacter E: Role of carbohydrates in oxidative modification of fibrinogen and other plasma proteins. *Arch Biochem Biophys* 321:175–181, 1995
5. Shacter E, Williams JA, Lim M, *et al*: Differential susceptibility of plasma proteins to oxidative modification: Examination by western blot immunoassay. *Free Radic Biol Med* 17:429–437, 1994
6. Sogami M, Nagoka S, Era S, *et al*: Resolution of human mercapt- and nonmercaptalbumin by high-performance liquid chromatography. *Int J Pept Protein Res* 24:96–103, 1984
7. Sogami M, Era S, Nagaoka S, *et al*: HPLC-studies on nonmercaptmercapt conversion of human serum albumin. *Int J Pept Protein Res* 25:398–402, 1985
8. Peters T, Jr.: *All About Albumin. Biochemistry, Genetics, and Medical Applications*, New York, Academic Press, 1996, pp 9–75
9. Janatova J, Fuller JK, Hunter MJ: The heterogeneity of bovine albumin with respect to sulfhydryl and dimer content. *J Biol Chem* 243:3612–3622, 1968
10. Noel JK, Hunter MJ: Bovine mercaptalbumin and nonmercaptalbumin monomers. Interconversions and structural differences. *J Biol Chem* 247:7391–7406, 1972
11. Wallevik K: SS-interchanged and oxidized isomers of bovine serum albumin separated by isoelectric focusing. *Biochim Biophys Acta* 420:42–56, 1976
12. Hayakawa A, Kuwata K, Era S, *et al*: Alteration of redox state of human serum albumin in patients under anesthesia and invasive surgery. *J Chromatogr B Biomed Sci Appl* 698:27–33, 1997
13. Sogami M, Era S, Nagaoka S, *et al*: High-performance liquid chromatographic studies on non-mercapt in equilibrium with mercapt conversion of human serum albumin. II. *J Chromatogr* 332:19–27, 1985
14. Suzuki E, Yasuda K, Takeda N, *et al*: Increased oxidized form of human serum albumin in patients with diabetes mellitus. *Diabetes Res Clin Pract* 18:153–158, 1992
15. Soejima A, Kaneda F, Manno S, *et al*: Useful markers for detecting decreased serum antioxidant activity in hemodialysis patients. *Am J Kidney Dis* 39:1040–1046, 2002
16. Fishbane S, Maesaka JK: Iron management in end-stage renal disease. *Am J Kidney Dis* 29:319–333, 1997
17. Macdougall IC, Chandler G, Elston O, *et al*: Beneficial effects of adopting an aggressive intravenous iron policy in a hemodialysis unit. *Am J Kidney Dis* 34:S40–S46, 1999
18. Mocks J: Cardiovascular mortality in haemodialysis patients treated with epoetin beta—A retrospective study. *Nephron* 86:455–462, 2000
19. Halliwell B: Superoxide-dependent formation of hydroxyl radicals in the presence of iron salts. Its role in degradation of hyaluronic acid by a superoxide-generating system. *FEBS Lett* 96:238–242, 1978
20. Rooyakkers TM, Stroes ES, Kooistra MP, *et al*: Ferric saccharate induces oxygen radical stress and endothelial dysfunction in vivo. *Eur J Clin Invest* 32(Suppl 1):9–16, 2002
21. Tovbin D, Mazor D, Vorobiov M, *et al*: Induction of protein oxidation by intravenous iron in hemodialysis patients: Role of inflammation. *Am J Kidney Dis* 40:1005–1012, 2002
22. Hayashi T, Era S, Kawai K, *et al*: Observation for redox state of human serum and aqueous humor albumin from patients with senile cataract. *Pathophysiology* 6:237–243, 2000
23. Climent I, Tsai L, Levine RL: Derivatization of gamma-glutamyl semialdehyde residues in oxidized proteins by fluoresceinamine. *Anal Biochem* 182:226–232, 1989
24. Schagger H, von Jagow G: Tricine-sodium dodecyl sulfate-polyacrylamide gel electrophoresis for the separation of proteins in the range from 1 to 100 kDa. *Anal Biochem* 166:368–379, 1987

25. HALLIWELL B, GUTTERIDGE JM: The antioxidants of human extracellular fluids. *Arch Biochem Biophys* 280:1-8, 1990
26. FERI B, STOCKER R, AMES BN: Small molecule antioxidant defenses in human extracellular fluids, in *The Molecular Biology of Free Radical Scavenging*, edited by Scandalios J, Cold Spring Harbor, Cold Spring Harbor Laboratory Press, 1992, pp 23–45
27. BERLETT BS, STADTMAN ER: Protein oxidation in aging, disease, and oxidative stress. *J Biol Chem* 272:20313–20316, 1997
28. DEAN RT, FU S, STOCKER R, *et al*: Biochemistry and pathology of radical-mediated protein oxidation. *Biochem J* 324(Pt 1):1-18, 1997
29. RADI R, BECKMAN JS, BUSH KM, *et al*: Peroxynitrite oxidation of sulfhydryls. The cytotoxic potential of superoxide and nitric oxide. *J Biol Chem* 266:4244–4250, 1991
30. FINCH JW, CROUCH RK, KNAPP DR, *et al*: Mass spectrometric identification of modifications to human serum albumin treated with hydrogen peroxide. *Arch Biochem Biophys* 305:595–599, 1993
31. SORIANI M, PIETRAFORTE D, MINETTI M: Antioxidant potential of anaerobic human plasma: Role of serum albumin and thiols as scavengers of carbon radicals. *Arch Biochem Biophys* 312:180–188, 1994
32. STAMLER JS, SIMON DI, OSBORNE JA, *et al*: S-nitrosylation of proteins with nitric oxide: Synthesis and characterization of biologically active compounds. *Proc Natl Acad Sci USA* 89:444–448, 1992
33. DEMASTER EG, QUAST BJ, REDFERN B, *et al*: Reaction of nitric oxide with the free sulfhydryl group of human serum albumin yields a sulfenic acid and nitrous oxide. *Biochemistry* 34:11494–11499, 1995
34. ZHANG H, MEANS GE: S-nitrosation of serum albumin: Spectrophotometric determination of its nitrosation by simple S-nitrosothiols. *Anal Biochem* 237:141-144, 1996
35. GATTI RM, RADI R, AUGUSTO O: Peroxynitrite-mediated oxidation of albumin to the protein-thiyl free radical. *FEBS Lett* 348:287–290, 1994
36. ANRAKU M, KRAGH-HANSEN U, KAWAI K, *et al*: Validation of the chloramine-T induced oxidation of human serum albumin as a model for oxidative damage in vivo. *Pharm Res* 20:684-692, 2003
37. FOLEY RN, PARFREY PS, SARNAK MJ: Clinical epidemiology of cardiovascular disease in chronic renal disease. *Am J Kidney Dis* 32:S112–S119, 1998
38. BARTFAY WJ, BUTANY J, LEHOTAY DC, *et al*: A biochemical, histochemical, and electron microscopic study on the effects of iron-loading on the hearts of mice. *Cardiovasc Pathol* 8:305–314, 1999
39. FELDMAN HI, SANTANNA J, GUO W, *et al*: Iron administration and clinical outcomes in hemodialysis patients. *J Am Soc Nephrol* 13:734–744, 2002
40. DRUEKE T, WITKO-SARSAT V, MASSY Z, *et al*: Iron therapy, advanced oxidation protein products, and carotid artery intima-media thickness in end-stage renal disease. *Circulation* 106:2212–2217, 2002
41. DESCAMPS-LATSCHA B, WITKO-SARSAT V: Importance of oxidatively modified proteins in chronic renal failure. *Kidney Int* 59:108–113, 2001
42. BOAZ M, SMETANA S, WEINSTEIN T, *et al*: Secondary prevention with antioxidants of cardiovascular disease in endstage renal disease (SPACE): Randomised placebo-controlled trial. *Lancet* 356:1213–1218, 2000
43. ROOB JM, KHOSCHSORUR G, TIRAN A, *et al*: Vitamin E attenuates oxidative stress induced by intravenous iron in patients on hemodialysis. *J Am Soc Nephrol* 11:539–549, 2000

Binding of α_1-Acid Glycoprotein to Membrane Results in a Unique Structural Change and Ligand Release

Koji Nishi,[‡] Toru Maruyama,[‡] H. Brian Halsall,[§] Tetsuro Handa,[||] and Masaki Otagiri*[,‡]

Graduate School of Pharmaceutical Science, Kumamoto University, 5-1 Oe-honmachi, Kumamoto 862-0973, Japan, Department of Chemistry, University of Cincinnati, Cincinnati, Ohio 45221-0172, and Graduate School of Pharmaceutical Sciences, Kyoto University, 46-29 Yoshida Shimoadachi-cho, Sakyo-ku, Kyoto 606-8501, Japan

Received March 31, 2004; Revised Manuscript Received May 25, 2004

ABSTRACT: α_1-Acid glycoprotein (AGP) consists of 183 amino acid residues and 5 carbohydrate chains and binds to basic and neutral drugs as well as steroid hormones. We investigated the structural properties and ligand-binding capacity of AGP under mild acidic conditions and its interactions with liposomes prepared from neutral or anionic lipids and the neutral drug, progesterone. Interestingly, AGP had a unique structure at pH 4.5, at which the tertiary structure changed, whereas the secondary structure remained intact. Furthermore, the binding capacity of AGP for progesterone did not significantly change under these conditions. It was also observed that AGP was strongly bound to the anionic membrane at pH 4.5, forming an α-helix-rich structure from the original β-sheet-rich structure, which significantly decreased the binding capacity of AGP for progesterone. The structural transitions as well as the membrane binding were suppressed by adding NaCl. These results indicate that AGP has a unique structure on the membrane surface under mild acidic conditions. The conformational change induces binding to the membrane aided by electrostatic interaction, and AGP subsequently takes on a predominantly α-helical conformation.

α_1-Acid glycoprotein (AGP),[1] a member of the lipocalin family, is a polypeptide with two disulfide bonds and five carbohydrate chains, which account for about 40% of its total mass of 36 kDa (*1*). It is a major binding protein for neutral and basic ligands (*2*−*5*). Although the three-dimensional structure and biological functions are still unknown, circular dichroism measurements (*6*) and molecular modeling (*7*) have revealed that this protein has a largely β-sheet structure in aqueous solution.

The hypothesis that membrane transport of a drug depends on the nonbound drug concentration is widely accepted. However, because this hypothesis does not fully explain the uptake mechanism of some AGP-binding drugs, a protein-mediated uptake system has been proposed (*8*−*11*). In such a system, structural changes in the protein due to interaction with the membrane surface decrease the drug-binding capacity. The recent ESR spectroscopic finding that the structure of HSA changes after interaction with the surface of hepatocytes supports this proposed system (*12*). It was recently reported that AGP binds to the vascular endothelial cell surface and then causes transcytosis across the cell without passing the intercellular junction (*13*). Andersen detected AGP on the surface of human monocytes, granulocytes, and lymphocytes using fluorescent electron microscopy (*14*, *15*). Other studies of AGP interacting with vesicles (*16*) and liposomes (*17*) also support the conclusion that AGP interacts with the membrane in circulation and may influence intracellular events. Furthermore, the oligosaccharide moiety of AGP is recognized by cell surface lectins (*18*).

We previously reported that the interaction between AGP and a biomembrane model (reverse micelles) resulted in structural change and a decrease in ligand-binding capacity. Moreover, this interaction resulted in a unique conformational transition: β-sheet to α-helix (*19*). Based on these results, it is important to investigate the structural properties and ligand-binding capacity of AGP under mild acidic conditions because local changes in pH on the biomembrane surface influence these parameters (*20*). Indeed, there are several reports that proteins undergo structural and functional changes under mild acidic conditions on the membrane surface and intracellularly (*21*−*23*), including other lipocalins (*24*).

In the present paper, we examined the relationship between structural properties under mild acidic conditions and the ability of AGP to interact with phospholipid interfaces containing neutral and anionic phospholipids. We demonstrate that AGP undergoes a unique conformational change under mild acidic conditions and that this conformational change promotes an interaction with the membrane. The ligand is then released due to either a change in affinity or closer membrane association. The process is a potentially useful model for studying the pharmacokinetics of both endogenous and exogenous substance binding to AGP and for elucidating further functions of AGP.

* To whom correspondence should be addressed. Tel: 81-96 371-4150. Fax: 81-96 362-7690. E-mail: otagirim@gpo.kumamoto-u.ac.jp.

‡ Kumamoto University.

§ University of Cincinnati.

|| Kyoto University.

[1] Abbreviations: AGP, α_1-acid glycoprotein; HSA, human serum albumin; PC, L-α-phosphatidylcholine; PG, L-α-phosphatidyl-DL-glycerol; PS, L-α-phosphatidyl-L-serine; PE, L-α-phosphatidyl ethanolamine; CD, circular dichroism; PAI-1, plasminogen activator inhibitor 1.

10.1021/bi0400204 CCC: $27.50
Published on Web 07/22/2004

MATERIALS AND METHODS

Materials. AGP (Cohn fraction VI), progesterone, L-α-phosphatidylcholine (PC) and ethanolamine (PE) from egg yolks, L-α-phosphatidyl-L-serine (PS) from bovine brain, and L-α-phosphatidyl-DL-glycerol sodium salt (PG) were all from Sigma Chemical Co. (St. Louis, MO). All other chemicals and solvents were of analytical grade.

Liposome Preparation. Liposomes were prepared as described previously (*25*). Briefly, phospholipids were dissolved in chloroform, and the solvent was evaporated under a stream of nitrogen and then under vacuum for at least 1 h. The phospholipid film was dispersed in the following 20 mM buffers: sodium phosphate (pH 6.0−7.4) and sodium acetate (pH 4.5−5.5), each containing 0−150 mM NaCl. Small unilamellar vesicles were prepared by sonication with a probe sonicator to near optical clarity, and residual multilamellar vesicles and titanium particles released from the probe were removed by centrifugation at 14000*g* for 20 min. Vesicles were mixed with AGP in the buffer at a final concentration of 10 mM AGP and 50−600 μM phospholipids (1:5−1:60 molar ratio of protein to phospholipids), and samples were incubated at room temperature for at least 1 h.

Measurement of Circular Dichroism Spectra. Circular dichroism spectra were recorded with a Jasco J-720 spectropolarimeter, using 10 μM AGP in 20 mM buffer (described above) at each pH. UV spectra were recorded in 10 mm and in 1 mm path length cells for near- and far-UV spectra, respectively.

Measurement of Fluorescence Spectra. Fluorescence was measured using a Jasco FP-770 fluorometer (Tokyo). AGP was dissolved at 10 μM in appropriate buffers. For Trp fluorescence, the excitation wavelength was 280 nm, and emission was monitored from 300 to 400 nm. ANS was added to a final concentration of 20 μM (2:1 molar ratio of ANS to AGP), which was enough to form the complex of AGP−ANS as much as possible and prevent nonspecific binding because it was reported that AGP had a high-affinity site for ANS (*25*). Spectra were recorded immediately after mixing. The excitation wavelength was 380 nm, and emission was monitored from 450 to 550 nm.

Membrane-Binding Experiment. Sucrose-loaded large unilamellar vesicles were prepared as previously described (*26*). The buffers (20 mM) used at each pH were as described above. Repeating the experiment with various buffers showed that the results depended on pH and not the buffer used. After incubation for 10 min at room temperature, solutions were centrifuged (20000*g*, 30 min) to separate vesicles and associated protein (pellet) from soluble protein (supernatant). Control experiments at all pH values showed that, in the absence of phospholipid vesicles, no AGP was present in the pellet after centrifugation. Samples were analyzed by the Bradford assay.

Progesterone−AGP-Binding Experiment. Binding of progesterone to AGP was determined by the ultrafiltration method. Progesterone was dissolved as 1 mg/mL in acetonitrile, and the stock solution was diluted with 20 mM sodium phosphate buffer (pH 6.0−7.4) and sodium acetate buffer (pH 4.5−5.5). The final concentration of acetonitrile did not exceed 1%. AGP solution (1 mL) containing progesterone was incubated for 10 min on ice and then centrifuged at 2000*g* for 40 min at 4 °C. After centrifugation, the filtrate (10 μL) was analyzed by HPLC to determine the free progesterone concentration. The HPLC system consisted of a Hitachi 655A-11 pump (Hitachi, Tokyo) and a Hitachi L-4000 UV detector set at 244 nm. The analytical column used was an AM312 ODS column (150 × 6.0 mm i.d., S-5 mm, 120 Å) (YMC, Kyoto) and was maintained at room temperature. The mobile phase was acetonitrile−20 mM sodium phosphate buffer (pH 7.4) (50:50 v/v) at a flow rate of 1 mL/min. AGP and PG concentrations were 10 and 400 μM, respectively. AGP−progesterone-binding experiments in the presence of liposomes had a final progesterone concentration of 10 μM (1:1 molar ratio of progesterone to AGP) after the liposomes had been saturated in progesterone to limit its nonspecific adsorption by the liposomes.

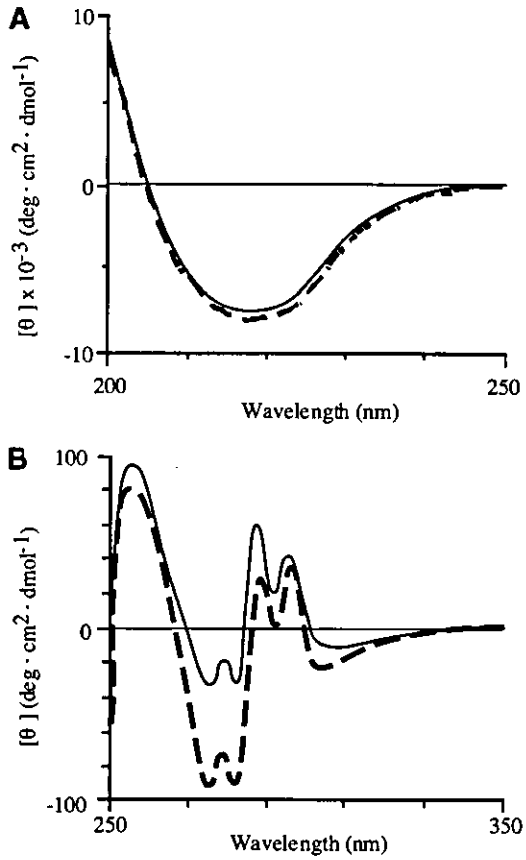

FIGURE 1: Effects of pH on the far-UV (A) and near-UV (B) CD spectra of AGP at pH 7.4 and 4.5, AGP spectra are shown as a continuous line (pH 7.4) and a dashed line (pH 4.5). Circular dichroism spectra were recorded using 10 μM AGP in a solution containing 20 mM buffer: sodium phosphate (pH 7.4) or sodium acetate (pH 4.5).

RESULTS

Effects of pH on the Conformational Structure of AGP. It has been reported that the pH at the membrane surface is lowered due to the membrane potential (*20*). This pH decrease may mediate interactions between proteins and the membrane itself (*24*). We investigated how the tertiary and secondary structures of AGP were affected under mild acidic conditions (pH 4.5−6.5) using circular dichroism spectroscopy (Figure 1). The tertiary structure changed slightly compared with that at pH 7.4, but the secondary structure was unaffected, even at pH 4.5. To obtain more information about the conformational changes in AGP under mild acidic

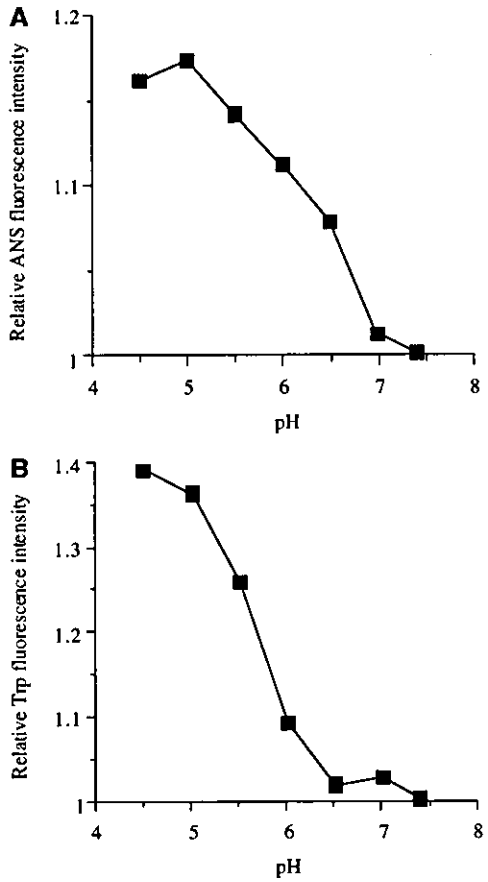

FIGURE 2: Fluorescence spectra of ANS and Trp residues at various pHs. AGP was dissolved at 10 μM in the appropriate buffers, and ANS was added to a final concentration of 20 μM (2:1 molar ratio of ANS to AGP). ANS: excitation wavelength, 380 nm; Trp: excitation wavelength, 280 nm.

conditions, we measured the fluorescence spectra of ANS and Trp residues on AGP at pH 4.5−7.4 (Figure 2). ANS is often used to evaluate hydrophobic regions, which are generally in the protein interior (*25*, *27*, *28*). The fluorescence intensity of ANS and Trp residues increased with lowering of pH. These results indicate that AGP has a unique conformational structure under the mild acidic conditions of the membrane surface, even in the absence of direct interactions between AGP and the membrane.

Effects of pH and NaCl on the AGP−Membrane Binding. The membrane environment has been shown to have a negative charge, in addition to being mildly acidic (*20*). We therefore examined the binding of AGP to PG- and PC-based membranes at each pH (pH 4.5−7.4) (Figure 3A). AGP bound strongly to the PG−membrane with lower pH, whereas significant binding was not observed with the PC−membrane at any pH. To confirm the presence of electrostatic forces in this interaction, the effects of NaCl on this binding were examined with the PG−membrane at pH 4.5 (Figure 3B). NaCl suppressed binding in a concentration-dependent manner (0 mM, 96.0 ± 0.58%; 75 mM, 37.5 ± 2.64%; and 150 mM, 10.0 ± 16.3%). The finding that other cations, Ca^{2+} and K^+, also inhibited the interaction between AGP and membrane suggests the presence of electrostatic force (data not shown). The above interaction was also observed even in physiological buffer, but it was small, as expected from the NaCl effect. To test the validity of this model and

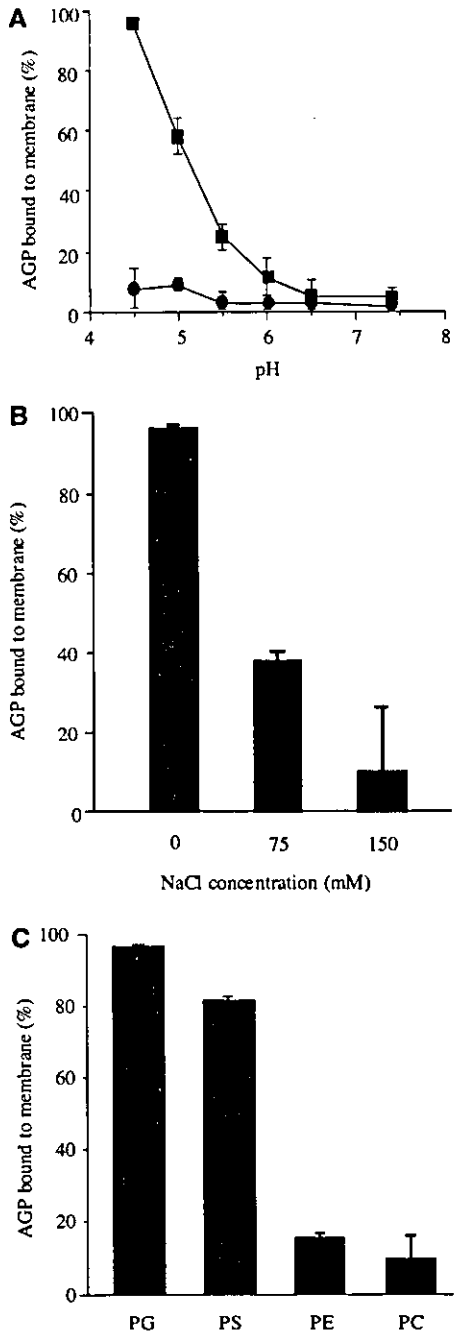

FIGURE 3: Interaction mode of AGP−membrane binding. (A) pH dependence of AGP binding to the membrane [PC (●), PG (■)]. (B) Effect of NaCl on the binding of AGP to the membrane. (C) Binding of AGP to the membrane made from other phospholipids. Experiments were performed using 10 μM AGP in solutions containing 20 mM buffers as described in Materials and Methods. Phospholipid vesicles were prepared at 400 μM.

experiment, the binding experiment was repeated using other phospholipids: PS and PE (Figure 3C). PG, PS, and PE (the degree of the negative charge: PG > PS > PE) are anionic lipids, PC is neutral, and the pattern of interaction of AGP with the lipids also supported the existence of an electrostatic interaction between AGP and the membrane. Moreover, at each pH, binding of AGP to PG−membrane had a significant correlation with the fluorescence intensity of Trp residues ($r = 0.9901$, $p < 0.01$) (Figure 4) but not ANS (data not shown). These results strongly suggest that the slight changes in AGP conformation observed under mild acidic conditions

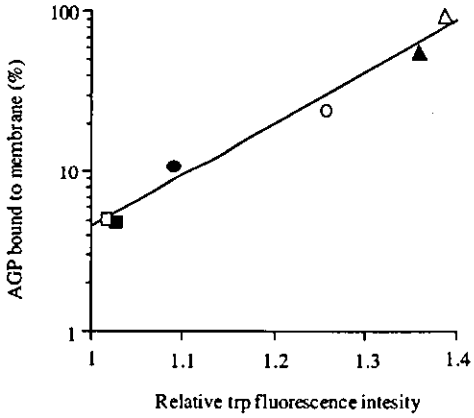

FIGURE 4: Correlation between AGP–membrane interaction and Trp residues of the AGP environment under mild acidic conditions. Each symbol represents the following pH: (■) 7.0, (□) 6.5, (●) 6.0, (○) 5.5, (▲) 5.0, and (△) 4.5.

lead to the binding of AGP to the membrane. This interaction may involve an electrostatic component.

Effects of pH and NaCl on the Conformation of AGP in Membrane Interactions. To evaluate the structural properties of AGP in membrane interactions, we examined the effects of pH and NaCl on the conformation of AGP in the presence of a PG–membrane (Figure 5). Panels B–D of Figure 5 show a $-[\theta]$ value of 222 nm as an index of the α-helix content. The secondary structure of AGP shifted from being β-sheet-rich to an α-helix-rich structure at lower pH (Figure 5A,B). In addition, the degree of this conformational transition depended on the PG concentration (Figure 5C) and was inhibited by higher NaCl concentrations (Figure 5D). These results indicated that this conformational transition was initiated following, or during, binding of AGP to the membrane.

Effects of Ligand-Binding Capacity of AGP in Membrane Interaction. It is important to understand how the ligand-binding capacity of AGP changes when the structural transition (β-sheet to α-helix) occurs in the presence of the PG–membrane. We used a representative AGP-binding ligand, progesterone, because it is uncharged and therefore unaffected by pH. The binding of progesterone to AGP had a good correlation with the α-helix content of AGP interacting with the PG–membrane at pH 4.5–7.4 ($r = 0.9545$, $p < 0.01$) (Figure 6). No changes in binding capacity were observed for pH 4.5–7.4 in the absence of PG–membrane. These results show that the binding of progesterone to AGP was strongly affected by its interaction with the PG–membrane but was not affected by mild acidic conditions.

DISCUSSION

The hypothesis that uptake of a drug depends on the free drug concentration (not bound by protein) is widely accepted. However, a pharmacokinetic study using albumin- and AGP-binding ligands found that uptake is more efficient than predicted by this model (*8*). One explanation for this phenomenon is that structural changes in the carrier protein may be induced by interaction with the target cell surface. Consequently, the ligand is released concomitantly with conformational changes in the protein (*8*–*11*). This idea is supported by ESR spectroscopic findings showing that albumin undergoes structural changes when interacting with hepatocytes (*12*). It should also be noted that AGP binds to

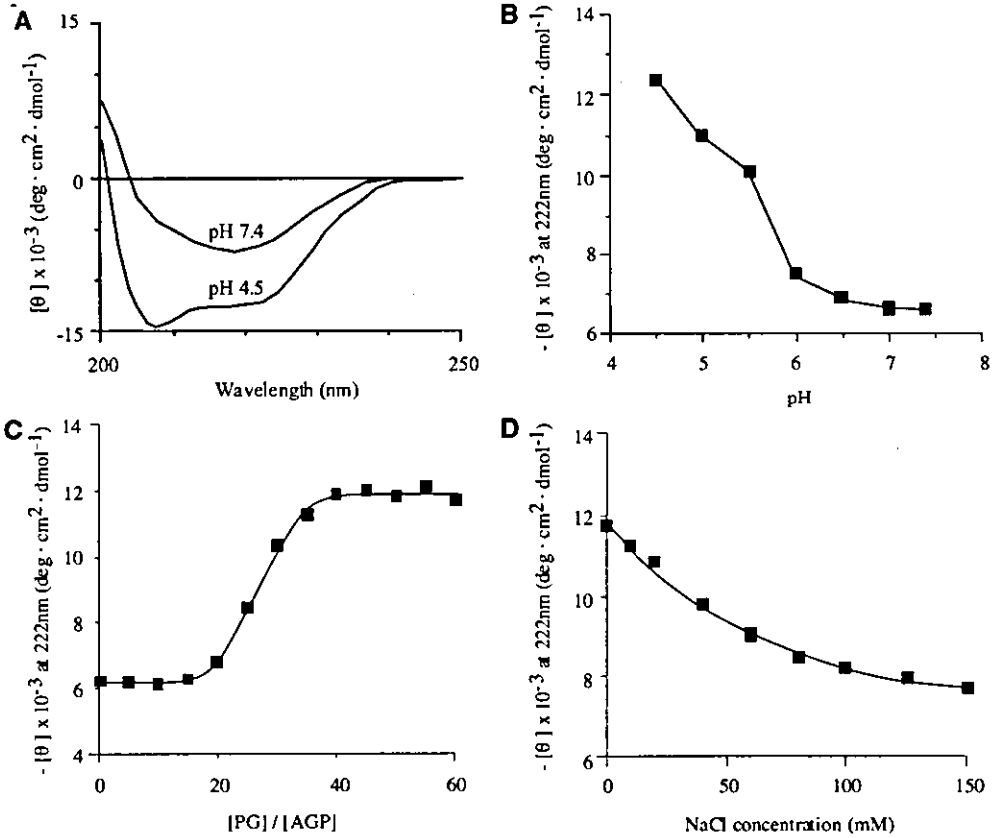

FIGURE 5: Effect of pH (A, B), PG concentration (C), and NaCl (D) on the conformational transition of AGP interacting with the membrane. Experiments were performed using 10 μM AGP in solution containing 20 mM buffer as described in Materials and Methods. The pH was 4.5 or 7.4 (A), was varied from 4.5 to 7.4 (B), or was 4.5 (C, D). Phospholipid vesicles were prepared at 400 μM (A, B, and D).

Table 1. Effects of *n*-Alkyl *p*-ABEs on the Number of Binding Sites (n) and Association Constant (K) for Primary DNSA Binding to HSA at pH 7.4

Type of *n*-alkyl *p*-ABE	$\frac{[n\text{-Alkyl } p\text{-ABEs}]}{[HSA]}$	n	K ($\times 10^5$ M^{-1})
None	0	1.07 ± 0.10	1.81 ± 0.37
Ethyl *p*-ABE	10	0.98 ± 0.15	1.94 ± 0.41
n-Propyl *p*-ABE	10	1.00 ± 0.15	1.92 ± 0.39
	2	1.11 ± 0.13	1.89 ± 0.42
	4	1.01 ± 0.11	1.84 ± 0.33
n-Buthyl *p*-ABE	6	0.98 ± 0.07	1.92 ± 0.25
	8	1.07 ± 0.17	1.82 ± 0.34
	10	1.03 ± 0.15	1.83 ± 0.15
n-Amyl *p*-ABE	10	1.13 ± 0.13	1.87 ± 0.37

The following concentrations were used to estimate the association constant of DNSA: HSA, 40 μM; DNSA, 4–40 μM. Data represent the mean ± SD of three experiments.

viscosity gave a straight line with a good correlation coefficient of 0.999. According to this finding, restriction of fluorescent probe mobility is accompanied by increased fluorescence anisotropy. Addition of increasing concentrations of *n*-butyl *p*-ABE to DNSA-HSA enhanced the fluorescence anisotropy of bound DNSA (Fig. 6). Actually, addition of high concentrations of all the *n*-alkyl *p*-ABEs increased the fluorescence anisotropy, and the mobility restriction of bound DNSA increased linearly with the number of carbon atoms in the alkyl side chain (Fig. 6A, inset). Increments of pH also resulted in enhanced fluorescence anisotropy of bound DNSA, but it did so in a less uniform way: changing pH from 6 to 8 increased fluorescence anisotropy, whereas an additional change to 9 resulted in a small reduction of fluorescence anisotropy (Fig. 6B). The latter finding indicates similar fluorescent probe mobilities at pH 8 and 9.

In summary, the fluorescence anisotropy data were more in agreement with the CD data than with the association constant data. This is especially evident when studying the effect of adding *n*-alkyl *p*-ABEs. These similarities between the CD and fluorescence anisotropic findings might be related to DNSA mobility at the binding region Ib.

Table 2. Effect of pH on the Number of Binding Sites (n) and Association Constant (K) for Primary DNSA Binding to HSA

pH	n	K ($\times 10^5$ M^{-1})
6.0	0.98 ± 0.12	1.37 ± 0.36
7.0	1.11 ± 0.20	1.66 ± 0.25
7.4	1.07 ± 0.15	1.81 ± 0.27
8.0	0.98 ± 0.13	2.95 ± 0.42
9.0	1.03 ± 0.09	4.11 ± 0.40

The following concentrations were used to estimate the association constant of DNSA: HSA, 40 μM; DNSA, 4–40 μM. Data represent the mean ± SD of three experiments.

DISCUSSION

HSA and α_1-acid glycoprotein (AGP) are two important transport and depot proteins in the circulation. AGP is considered to possess only one ligand binding site, consisting of several overlapping regions for exogenous and endogenous substances.[28] HSA has at least three binding sites for high-affinity binding of drugs, namely, site I, site II and site III also called the warfarin,

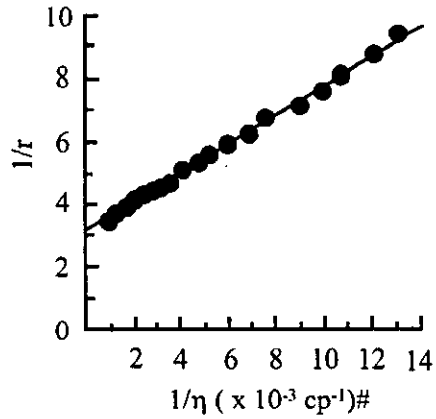

Figure 5. Relation between medium viscosity (η) and DNSA fluorescence anisotropy (r). The relationship is shown in a double reciprocal plot. The correlation coefficient is 0.999. The viscosity of glycerol as a medium is adjusted by temperature changes. #Viscosity is given as centipoise (cp).

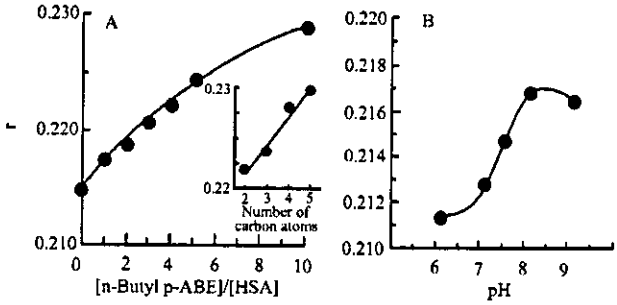

Figure 6. Effects of *n*-butyl *p*-ABE (A) and pH (B) on the fluorescence anisotropy (r) of DNSA bound to HSA. The following concentrations were used for HSA and DNSA: HSA, 40 μM; DNSA, 10 μM. The concentration of *n*-butyl *p*-ABE is represented as the molar ratio to HSA in (A). The inset to (A) indicates the effect of the number of carbon atoms in the *n*-alkyl *p*-ABEs at an *n*-alkyl *p*-ABEs to HSA molar ratio of 10. The experiments of (A) were performed at pH 7.4.

benzodiazepine and digitoxin binding site, respectively.[4–6] At the molecular level, the binding sites of HSA may also consist of several binding regions.[14–17,19] In other words, a binding site might be composed of a group of several regions which are adjacent to or overlapping each other. For example, site I is thought to consist of two (warfarin and azapropazone binding regions)[14] or three regions (regions Ia, Ib, and Ic).[19] In addition, because of differences in bilirubin-displacing effects[15] and in stereoselective binding modes,[16,17] drug binding indicates that also site II can be subdivided into binding regions.

Mutual displacement of drugs is often the result of competitive binding to a site or region at a drug carrier protein. Although drugs that bind to different sites or regions cannot interact directly according to a competitive binding model, indirect effects such as cooperative or anticooperative interaction may change drug binding. For example, the interaction between AGP-bound dicoumarol derivatives and protriptyline has been suggested to be the result of such binding modes.[29] This type of finding leads us to the idea that even though the binding constants for two ligands, as determined by, for example, equilibrium dialysis, are not affected by simultaneous binding, the binding could still be influenced by conformational changes in the protein. For testing this hypothesis, we have studied cobinding of DNSA and *n*-alkyl *p*-ABEs to site I of HSA by both equilibrium dialysis and spectroscopic techniques.

Interaction of HSA and DNSA, which is a probe for region Ib, generated a Cotton effect at around 360 nm at pH 7.4 (Fig. 2). Because unbound DNSA is not optically active, and HSA does not produce any Cotton effects at these wavelengths, the observed Cotton effects must be extrinsic in origin. The extrinsic Cotton effects are thought to result from interaction of ligand chromophore with an asymmetrical locus in the protein.[30–33] Thus, extrinsic Cotton effects reflect the characteristics of specific asymmetrical sites in the protein molecule and could provide information on the microenvironment of binding sites or ligand orientation in the sites. Therefore, Cotton effects produced by the DNSA-HSA interaction are useful for investigating possible relations between region Ib and, for example, region Ic.

Equilibrium dialysis proposed independent binding of DNSA and the *n*-alkyl *p*-ABEs, which are probes for region Ic, at all pH values studied (Table 1 and data not shown). This finding is in accordance with previous analyses of equilibrium dialysis data performed with an equation that included different interaction modes (competitive, independent, cooperative, or anticooperative binding).[19] However, the results of the CD measurements revealed that binding of the *n*-alkyl *p*-ABEs changed the spatial relationship for bound DNSA (Fig. 2). Furthermore, the spectral changes were very similar to those accompanying increments in pH in the region, in which HSA is known to undergo the neutral-to-base transition (N-B transition). In accordance with these findings, the effect of *n*-alkyl *p*-ABEs binding on the CD spectra of the DNSA-HSA system was predominant at pH 6, whereas there was only a very small effect at pH 9 (Fig. 4). The magnitude of the effects of *n*-alkyl *p*-ABEs was dependent on the concentration of the ligand and on the length of the alkyl side chain. It is reasonable to consider that the DNSA molecule takes up the most preferable orientation in the B conformer, because maximal extrinsic Cotton effects were observed at pH 9, and addition of *n*-alkyl *p*-ABEs did not cause further effects on the spatial orientation of DNSA to the asymmetric center in the B conformer. Such a binding model is also in accordance with the finding that DNSA binds with a higher association constant at pH 9 (Table 2). The proposal that the N-to-B transition and *n*-alkyl *p*-ABEs binding cause reorientation of HSA-bound DNSA was supported by fluorescence polarization data, because fluorescence anisotropy derived from the DNSA-HSA complex gives information about the mobility of bound DNSA.[34] The results showed (Fig. 6) that the mobility of DNSA bound to HSA is restricted by

the N-B transition and *n*-alkyl *p*-ABE binding in a similar manner.

Within the pH range used, the association constant for DNSA binding to HSA describes a sigmoidal curve (Table 2, not illustrated). This finding is consistent with other studies using site I ligands.[20,35–37] Therefore, HSA is considered also to take up the N and B conformations at pH 6 and 9, respectively, when complexed with DNSA.

Despite the similarity of the effects of N-B transition and *n*-alkyl *p*-ABE binding on DNSA's spatial orientation, their effects on equilibrium binding, and thereby the binding constant for DNSA, were different. The N-B transition increased DNSA binding, whereas cobinding of the *n*-alkyl *p*-ABEs did not significantly affect DNSA binding. Based on studies with HSA fragments, domains I and II undergo dramatic changes in tertiary structure as the N-B transition proceeds.[38] The proton bindings and releases are considered to be involved in the process of the N-B transition.[35,39] The structural changes involving delayed deprotonation of five histidine residues in domain I and breaking of salt bridges between domains I and III cause increased flexibility of the HSA molecule and tighter binding of ligands to site I in subdomain IIA.[10,11,35,37,40,41] In addition to the N-B transition, HSA undergoes several other transitions in dependence of pH, namely, the N-F transition between pH 5.0 and 3.5 and the F-E transition or acid expansion below pH 3.[8,42] Among these structural transitions, the N-B transition has been proposed to have physiological importance, because it takes place within the pH range of blood plasma,[8,22,35,42,43] and could change not only individual binding of drugs but also ligand-ligand interactions on HSA through changes in spatial relationships between regions or sites.[22,44,45] It is somewhat surprising that, even though the N-B transition affects DNSA binding, it has no influence on the type of interaction between HSA-bound DNSA and *n*-alkyl *p*-ABE, namely, independent binding to site I. Thus, the changes of DNSA's spatial orientation in region Ib caused by the N-B transition and by *n*-alkyl *p*-ABE binding cannot be identical.

A possible scheme for the changes in DNSA's binding and spatial orientation is given in Figure 7. In short, at pH 6, DNSA binds with a relatively low affinity to region Ib; the binding results in a CD spectrum with positive θ values (upper left corner). Increasing pH to 9 modifies the conformation of the binding site which results in high-affinity binding and in a CD spectrum with maximal negative θ values (upper right corner). However, simultaneous binding of an *n*-alkyl *p*-ABE to region Ic at pH 6 does not affect the association constant for DNSA to a detectable degree but affects the orientation of bound DNSA. The latter effect results in a CD spectrum with moderate negative θ values (lower left corner). Finally, independent high-affinity binding of the two types of ligands also takes place at pH 9. Actually, the binding affinity and orientation of bound DNSA, as well as the CD spectrum, are the same, whether *n*-alkyl *p*-ABEs are present or not (lower right corner). For illustration clarity, we have not shown the fluorescence results which, however, are in accordance with the scheme. A final evaluation of the model probably has to be done by X-ray analyses of HSA-ligand crystals.

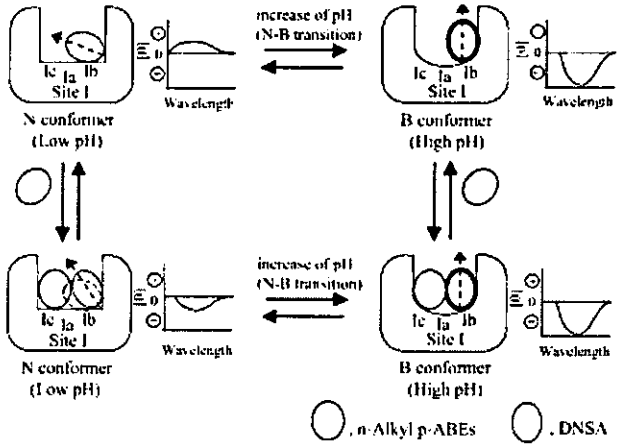

Figure 7. Schematic model of the change in spatial orientation of DNSA in region Ib and of its CD spectrum caused by binding of *n*-alkyl *p*-ABEs to region Ic at different pHs. The dashed arrows indicate the direction of contribution to positive or negative ellipticities on that orientation, and the bold line in the DNSA molecule indicates binding with high affinity.

In conclusion, the results showed that even though one method, for example, equilibrium dialysis, proposes independent binding of two ligands, other methods, for example, CD and fluorescence measurements, can detect interactions between the bound ligands. The results also showed that such interactions can be modulated by structural changes in the protein molecule, for example, those accompanying the N-B transition of HSA. The present findings afford a deep insight into drug binding to site I and a way of looking at a new type of interaction.

REFERENCES

1. Sellers EM, Koch-Weser J. 1977. Clinical implications of drug-albumin interaction. In: Rosenoer VM, Oratz M, Rothschild MA, editors. Albumin structure, function and uses. Oxford, UK: Pergamon Press, pp 159–182.
2. Vallner JJ. 1977. Binding of drugs by albumin and plasma protein. J Pharm Sci 66:447–465.
3. McMenamy RP. 1977. Albumin binding sites. In: Rosenoer VM, Oratz M, Rothschild MA, editors. Albumin structure, function and uses. Oxford, UK: Pergamon Press, pp 143–158.
4. Sudlow G, Birkett DJ, Wade DN. 1975. The characterization of two specific drug binding sites on human serum albumin. Mol Pharmacol 11:824–832.
5. Sudlow G, Birkett DJ, Wade DN. 1976. Further characterization of specific drug binding sites on human serum albumin. Mol Pharmacol 12:1052–1061.
6. Sjöholm I, Ekman B, Kober A, Ljungstedt-Pahlman I, Seiving B, Sjödin T. 1979. Binding of drugs to human serum albumin. XI. The specificity of three binding sites as studied with albumin immobilized in microparticles. Mol Pharmacol 16:767–777.
7. He XM, Carter DC. 1992. Atomic structure and chemistry of human serum albumin. Nature 358: 209–215.
8. Carter DC, Ho JX. 1994. Structure of serum albumin. Adv Protein Chem 45:153–201.
9. Petitpas I, Bhattacharya AA, Twine S, East M, Curry S. 2001. Crystal structure analysis of warfarin binding to human serum albumin: Anatomy of drug site I. J Biol Chem 276:22804–22809.
10. Bos OJ, Remijn JP, Fischer MJ, Wilting J, Janssen LH. 1988. Location and characterization of the warfarin binding site of human serum albumin. A comparative study of two large fragments. Biochem Pharmacol 37:3905–3909.
11. Bos OJ, Fischer MJ, Wilting J, Janssen LH. 1989. Mechanism by which warfarin binds to human serum albumin. Stopped-flow kinetic experiments with two large fragments of albumin. Biochem Pharmacol 38:1979–1984.
12. Dockal M, Carter DC, Ruker F. 1999. The three recombinant domains of human serum albumin. Structural characterization and ligand binding properties. J Biol Chem 274:29303–29310.
13. Dockal M, Chang M, Carter DC, Ruker F. 2000. Five recombinant fragments of human serum albumin-tools for the characterization of the warfarin binding site. Protein Sci 9:1455–1465.
14. Fehske KJ, Schlafer U, Wollert U, Müller WE. 1982. Characterization of an important drug binding area on human serum albumin including the high-affinity binding sites of warfarin and azapropazone. Mol Pharmacol 21:387–393.
15. Maruyama K, Nishigori H, Iwatsuru M. 1985. Characterization of the benzodiazepine binding site (diazepam site) on human serum albumin. Chem Pharm Bull 33:5002–5012.
16. Noctor TAG, Pham CD, Kaliszan R, Wainer IW. 1992. Stereochemical aspects of benzodiazepine binding to human serum albumin. I. Enantioselective high performance liquid affinity chromatographic examination of chiral and achiral binding interactions between 1,4-benzodiazepines and human serum albumin. Mol Pharmacol 42:506–511.
17. Kaliszan R, Noctor TAG, Wainer IW. 1992. Stereochemical aspects of benzodiazepine binding to human serum albumin. II. Quantitative relationships between structure and enantioselective retention in high performance liquid affinity chromatography. Mol Pharmacol 42:512–517.
18. Kragh-Hansen U. 1988. Evidence for a large and flexible region of human serum albumin possessing high affinity binding sites for salicylate, warfarin, and other ligands. Mol Pharmacol 34:160–171.
19. Yamasaki K, Maruyama T, Kragh-Hansen U, Otagiri M. 1996. Characterization of site I on human serum albumin: Concept about the structure of a drug binding site. Biochim Biophys Acta 1295:147–157.
20. Yamasaki K, Miyoshi T, Maruyama T, Takadate A, Otagiri M. 1994. Characterization of region Ic in site I on human serum albumin. Microenvironmental analysis using fluorescence spectroscopy. Biol Pharm Bull 17:1656–1662.
21. Sakai T, Yamasaki K, Sako T, Kragh-Hansen U, Suenaga A, Otagiri M. 2001. Interaction mechanism between indoxyl sulfate, a typical uremic toxin bound to site II, and ligands bound to site I of human serum albumin. Pharm Res 18:520–524.
22. Yamasaki K, Maruyama T, Yoshimoto K, Tsutsumi Y, Narazaki R, Fukuhara A, Kragh-Hansen U, Otagiri M. 1999. Interactive binding to the two principal ligand binding sites of human serum albumin: Effect of the neutral-to-base transition. Biochim Biophys Acta 1432:313–323.
23. Chen RF. 1967. Removal of fatty acids from serum albumin by charcoal treatment. J Biol Chem 242: 173–181.
24. Kadaba PK, Carr M, Tribo M, Triplett J, Glasser AC. 1969. Boron trifluoride ethyl ether as an effective catalyst in the synthesis of alkyl *p*-aminobenzoates. J Pharm Sci 58:1422–1423.
25. Dash D, Rao GR. 1990. Characterization of the effects of propranolol on the physical state of platelet membrane. Arch Biochem Biophys 276:343–347.
26. Chen RF, Bowman RL. 1965. Fluorescence polarization: Measurement with ultraviolet-polarizing filters in a spectrophotofluorometer. Science 147: 729–732.

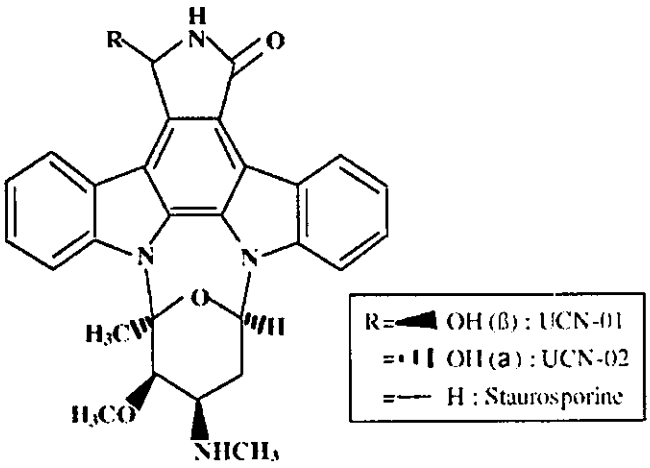

Fig. 1. Chemical structures of UCN-01, UCN-02 and staurosporine.

Since at present no crystallographic structural data for hAGP is available, it becomes important to examine the extraordinarily high affinity binding mechanism between UCN-01 and hAGP using established methods. In this study, we report on the binding interactions between UCN-01 and related compounds with native and chemically modified hAGP using ultracentrifugation and spectroscopic analysis to detect these interactions.

MATERIALS AND METHODS

Materials

UCN-01, UCN-02 and Staurosporine were supplied by Kyowa Hakko Kogyo Co. (Shizuoka, Japan). hAGP (purified from cohn fraction VI) was purchased from Sigma Chemical Co. (St. Louis, MO, USA). Phenylisocyanate and 2-hydroxy-5-nitrobenzyl bromide (HNBB) were purchased from Nacalai Tesque (Kyoto, Japan). Tetranitromethane (TNM) was purchased from Aldrich Chemical Co., Milwaukee, USA. Diethylpyrocarbonate (DEP) and neuraminidase was purchased from Sigma Chemical Co. All other chemicals and solvents were of analytical grade.

Determination of Binding Constant

The binding of UCN-01 to hAGP was determined by an ultracentrifugation technique (17). A constant concentration of hAGP (4 μM) was incubated with different concentrations of UCN-01 (3.2–8 μM). Five ml of an hAGP solution containing UCN-01 was placed in siliconized tubes, along with SIGMACOATE (Sigma), incubation for 10 min on ice, and then ultracentrifuged at 225,000 × g for 24 h at 4°C. After ultracentrifugation, an aliquot (50 μl) from the top of the supernatant was used to determine the free UCN-01 concentration by HPLC, as reported previously (18). The unbound fractions were obtained from the supernatant.

Binding parameters were determined by fitting the experimental data to the following Scatchard equation using a non-linear squares program (MULTI program) (19).

$$\frac{r}{D_f} = nK - rK \quad (1)$$

where n is the number of binding sites, K the binding constant, and D_f the free drug concentration, with r denoting the moles of bound ligand per mole of total protein.

Determination of Binding for UCN-01 to hAGP

Percent binding was calculated from the following equation:

$$\text{bound}\,(\%) = \frac{[D_t] - [D_f]}{[D_t]} \times 100 \quad (2)$$

where D_t is the total concentration of UCN-01, the hAGP concentrations were set at 20 μM, and D_f is the free concentration of UCN-01.

Preparation of hAGP Derivatives

Trp-Modified hAGP

The three Trp residues of hAGP were modified by HNBB following the procedure of Fehske *et al.* (20). 40 mg of hAGP was dissolved in 10 ml deionized water adjusted to pH 4.5 with acetic acid. One milliliter of an ethanol solution of HNBB was added to 10 ml of this solution. HNBB was added (100-fold molar excess of hAGP) and the reaction mixture was shaken occasionally. After 2 h the insoluble hydrolyzed reagent was separated by centrifugation. The supernatant was dialyzed against deionized water for 60 h and then lyophilized. The degree of modification was determined using ultraviolet absorption, as shown below.

$$\text{modified}\,(\%) = \frac{A_{410} \times 44100 \times 0.4980}{13800\,(A_{280} - 0.167 \times A_{410})} \times 100 \quad (3)$$

where A_{410} is the maximal absorbance of Trp-modified hAGP, and A_{280} is the maximal absorbance of unmodified hAGP. Of the 3 Trp residues of hAGP, about 1 was modified.

Tyr-Modified hAGP

Modification of the Tyr residues was performed at 4°C according to the procedure of Sokolovsky *et al.* (21). hAGP was dissolved in 10 ml of 0.05 M Tris buffer with a pH of 8.0. A 500-fold molar excess of TNM dissolved in ethanol was added to the hAGP solution. The degree of modification was calculated from the following equation:

$$\text{modified}\,(\%) = \frac{A_{428}}{4100 \times c \times m} \times 100 \quad (4)$$

where A_{428} is the maximal absorbance of Tyr-modified hAGP, c the protein concentration, and m the number of Tyr

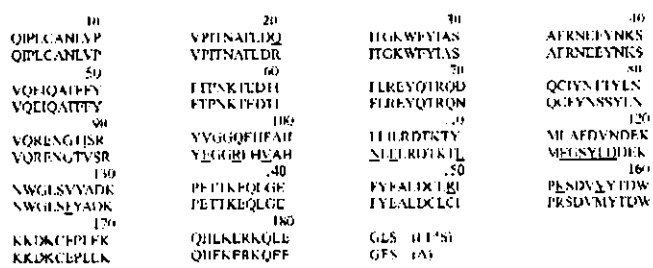

Fig. 2. Amino acid sequence of hAGP variants. Differences in the amino acid sequence between the F1*S and A variant are underlined.

residues on an hAGP molecule. Of the 11 Tyr residues of hAGP, about 2 were modified.

Lys-Modified hAGP

Chemical modification of Lys residues was carried out using phenylisocyanate (22). 40 mg of hAGP was dissolved in 10 mL 0.067 M phosphate buffer at pH 7.4. One milliliter of an ethanol solution of phenylisocyanate was added gradually at a 300-fold molar excess over hAGP and the reaction mixture was incubated for 2 h at 4°C, dialyzed against deionized water for 40 h, and then lyophilized. The unreacted Lys residues were determined by the trinitrobenzene sulfonic acid procedure of Haynes *et al.* (23). Of the 14 Lys residues of hAGP, about 4 were modified.

His-Modified hAGP

The His residues were modified with DEP according to the procedure of Roosemont *et al.* (24). 30 mg of hAGP was dissolved in 10 ml of acetate buffer (pH 6.5, 100 mM), DEP in ethanol was then added to the hAGP solution. The ratio of DEP to hAGP was 10. The mixture was stirred for 20 min at 4°C and dialyzed against deionized water and lyophilized. The number of His residues modified was calculated using the following equation:

$$\text{modified (\%)} = \frac{A_{240} \times \frac{3\text{ ml}}{\text{ml of test solution}}}{\Delta\varepsilon \times c \times m} \times 100 \qquad (5)$$

where $\Delta\varepsilon$ is the differential molar absorptivity for His at pH 6.0, c the protein concentration and m the number of His residues on hAGP. A_{240} is the maximal absorbance of His-modified hAGP. Of the 3 His residues in hAGP, about 2 were modified.

Separation of hAGP Genetic Variants

The hAGP genetic variants were separated using the method of Herve *et al.* (25). An iminodiacetate (IDA) Sepharose gel loaded with copper (II) ions and equilibrated in buffer 1 (20 mM sodium phosphate buffer, pH 7.0, containing 0.5 M sodium chloride) was packed into a glass column (2.0 × 30.0 cm L, Pharmacia LKB). Commercial hAGP (70 mg dissolved in 1.0 ml of buffer) was applied to the column at a flow rate of 1.0 ml/min. Fractions (10 ml) were collected, and their respective absorbance values were determined spectrometrically at 280 nm. As soon as variant A had been eluted, elution buffer 2 (buffer 1 plus 20 mM imidazole) was applied to the column to remove the bound F1 and S variants (F1/S mixture). The peak fractions of each eluent were collected, concentrated on a YM 10 membrane filter (Amicon, Danvers, MA), dialyzed against deionized water, and lyophilized. The purities of the isolated hAGP preparations were determined by isoelectric focusing (IEF) followed by incubation at 37°C for 24 h with 1 U of neuraminidase (25).

Desialylation of hAGP

hAGP was desialylated enzymatically, using the methodology described by Primozic and McNamara (26), using an immobilized neuraminidase obtained from *Clostridium perfringens*. hAGP (40 mg) was dissolved in 5 ml of 0.067 M phosphate buffer (pH 7.4) and 2 U of enzyme were added. The mixed solution was incubated at 37°C, with gentle stirring at 60 rpm for 24 h after incubation, the mixture was centrifuged and filtered to remove the immobilized enzyme. A small part of the filtrate was used to measure sialic acid by the thiobarbituric acid method. The product was dialyzed against deionized water and the dialysate was lyophilized. Approximately 95% of the sialic acid was removed, leaving an average of one sialic acid residue per protein molecule. The molecular weight of desialylated hAGP was therefore 40000.

Circular Dichroism (CD) Spectra

Circular dichroism spectra were recorded with a JASCO J-720 spectropolarimeter, using 10 μM hAGP in 20 mM buffer at 25°C. Near-UV spectra were recorded using a 10-mm path length cell, and a 0.1-mm path length cell was used for far–UV spectra. Prior to recording the spectra, samples were mixed by vortexing and then incubated for 30 min at room temperature. The mean residue ellipticity [θ], was calculated using the following equation:

$$[\theta] = \frac{\theta}{10 \times c \times 1} \qquad (6)$$

where θ (deg) is the observed ellipticity, l the cell length (cm).

$$c = nCp \qquad (7)$$

where n is the number of amino acid residues and Cp the concentration (mol/L).

Tryptophanyl Fluorescence Spectrum

Fluorescence was measured using a Jasco FP-770 fluorometer (Tokyo, Japan). The excitation wavelength of hAGP was 295 nm, and fluorescent wavelength, 340 nm. The relative fluorescence intensity was calculated using the fluorescence quenching method.

Statistical Analysis

All data are presented as means ± SD. Statistical analysis of difference was determined by one-way ANOVA followed by the modified Fisher's least sequares difference method.

RESULTS

Binding Parameter of UCN-01 Analogs to hAGP

UCN-01 is a novel derivative of staurosporine that is hydroxylated C-7, and UCN-02 is a stereoisomer at C-7 of UCN-01. UCN-01, UCN-02 and staurosporine have been shown to inhibit PKC with IC50 (μM) values of 0.0041, 0.062 and 0.0027, respectively, and to inhibit protein kinase A (PKA) with IC50 (μM) values of 0.042, 0.25, and 0.0082, respectively (27).

Table I shows the binding affinity constants, K_a, of UCN-01 analogues for hAGP. The K_a of UCN-01 for hAGP, 288 ± 75 × 10^6 M^{-1}, is the highest among the three compounds, and is in agreement with previously reported values (5). The K_a for staurosporine where hydrogen is the substituent at C-7 position is about one-twentieth. UCN-02 with an α-hydroxyl group at the C-7 position shows the smallest binding constant among the three ligands, compared to UCN-01. It is interest-

Table I. Binding Parameters of UCN-01, UCN-02, and Staurosporine to hAGP at pH 7.4

	Ligand		
	UCN-01	UCN-02	Staurosporine
K_a ($\times 10^6$ M^{-1})	288 ± 75	1.48 ± 0.11	11.33 ± 5.74
n	0.92 ± 0.04	0.93 ± 0.06	0.91 ± 0.11

All values are mean ± SD (n = 3).

ing to note that a change in the configuration of the hydroxyl group or a substitution of a hydrogen atom at the C-7 position of UCN-01 caused a 20- to 100-fold decrease in binding affinity.

Effect of pH on Binding of UCN-01 to hAGP

The binding of ligands to hAGP is known to be a pH sensitive process (28). The percentage of binding of UCN-01 to hAGP at different pHs, namely 6, 7, 7.4, and 8, was investigated (Fig. 3). The maximum binding of UCN-01 to hAGP occurs at pH 7.4 (96.33%). The binding of UCN-01 to hAGP was found to decrease in both acidic and basic pH values, where the lowest percentage binding was observed at pH 6 (69.74%).

Near-UV CD Spectra of hAGP in Various pHs

Structural profiles of hAGP at pH 6, 7, 7.4, and 8 were investigated by circular dichroism measurements. CD spectra measured at the near UV region reflects conformation or tertiary structure of a protein, while that measured at the far UV region reflects secondary structure. A change in the shape of a CD spectra measured under different conditions in comparison to a reference spectra of a particular set of conditions usually indicates a change in the conformation of the protein. The secondary structures of hAGP were essentially unchanged within the range of pH 6–8 (data not shown), but the tertiary structure changed significantly, as shown in the near UV CD spectra in Fig. 4. These results suggested that the conformational change in the tertiary structure of hAGP is pH dependent. Such a conformational change could affect the microenvironment of binding sites, thus causing a change in the binding of UCN-01 to hAGP.

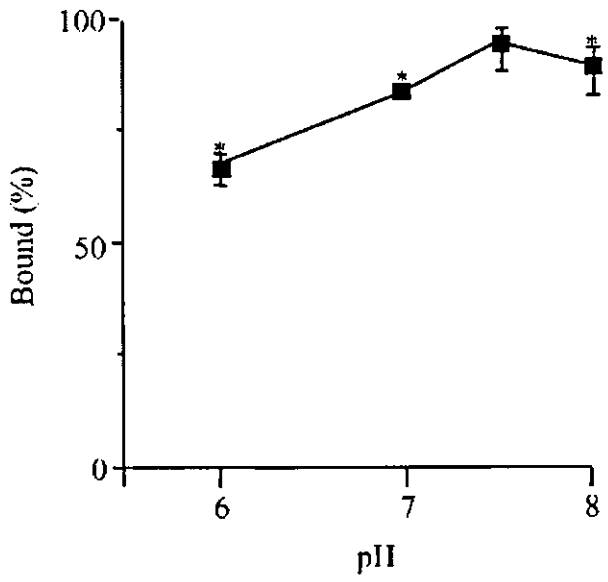

Fig. 3. Effect of pH on the binding of UCN-01 to hAGP. Concentrations are: [UCN-01] = [hAGP] = 20 μM. Each point represents the mean ± SD (n = 3). *Statistically significant compared with pH 7.4; $p < 0.01$.

Effect of Sialic Acid on the Binding of UCN-01 to hAGP at pH 7.4

The carbohydrate terminal chains of hAGP glycans are highly sialylated, containing up to 14 sialic acid residues (29). Therefore, hAGP has a low pKa (=2.6) and isoelectric point (=2.7). Sialic acid residues have been reported to influence the binding of several drugs to hAGP (30). In order to elucidate the role of sialic acid in the binding of UCN-01, we prepared desialylated hAGP and examined the binding percentage of UCN-01 to native and desialylated hAGP, which were 96.33 ± 1.26 and 95.59 ± 1.06, respectively. This suggested that the binding of UCN-01 to desialylated hAGP is comparable to that of native hAGP.

Binding Affinity of UCN-01 to hAGP Variants at pH 7.4

We separated the F1*S and A variants from the hAGP mixture and examined the percentage binding of UCN-01 to each of the variants. As shown in Table II, (the binding percentage of UCN-01 to native, F1*S and A variants are 96.33 ± 1.26, 95.08 ± 0.3 and 95.23 ± 0.45, respectively) there is no significant difference in the binding percent of UCN-01 to the F1*S and A variants of hAGP.

Near-UV CD Spectra of Chemical Modified hAGP and the Effects of the Chemical Modification on Binding of UCN-01 to hAGP

UCN-01 has a very high affinity to hAGP. This high affinity is thought to be derived from not only the hydrophobic interaction but also largely from the electrostatic interac-

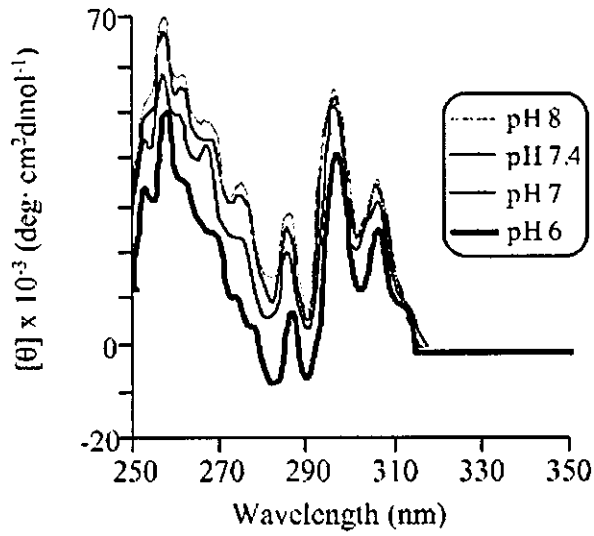

Fig. 4. Near-UV CD spectra of hAGP at various pHs The concentration is: [hAGP] = 10 μM.

Table II. Binding Percentage of UCN-01 to hAGP Variants at pH 7.4

	hAGP		
	Native	F1*S	A
Binding percentage (%)	96.33 ± 1.26	95.08 ± 0.3	95.23 ± 0.45

The concentrations are: [hAGP] = [F1*S] = [A] = [UCN-01] = 20 μM.
All values are means ± SD (n = 3).

tion between UCN-01 and hAGP. In actual fact, binding of UCN-01 to hAGP was affected by the presence of sodium chloride and fatty acid (data not shown). In order to evaluate the role of amino acid residues involved in the binding, we compared the binding of UCN-01 with chemically modified hAGPs. Chemical modification of His, Lys, Trp and Tyr residues of hAGP caused a marked decrease in the binding of UCN-01, with the modification of Trp residues showing the greatest extent of decrease (Table III). In addition, we also measured the binding percentage of staurosporine to these four chemically modified hAGPs and similar results were obtained where modification of Trp residues caused a marked decrease in the binding of staurosporine (data not shown). The CD spectra of His, Lys, Trp, and Tyr residues modified hAGP indicated that the secondary structure of all modified hAGPs hardly change (data not shown), but the tertiary structure changed significantly, particularly in the case of Trp residue modified hAGP (Fig. 5). The fluorescence quenching titration curve of UCN-01 binding to hAGP as shown in Fig. 6 indicated that tryptophan residues may play an important role in the binding of UCN-01 to hAGP.

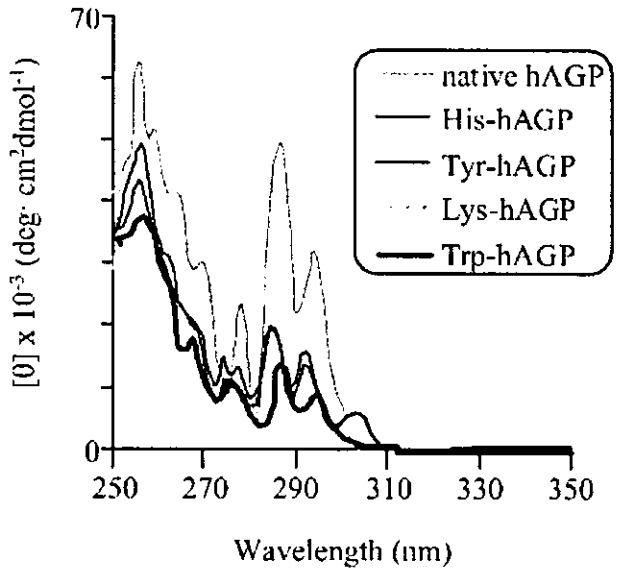

Fig. 5. Near-UV CD spectra of modified hAGPs at pH 7.4 The concentration is: [modified hAGPs] = 10 μM.

DISCUSSION

The initial treatment protocol for UCN-01 was a 72-h infusion administered at 2-week intervals. However, the clinical outcome of the first nine patients treated using this schedule demonstrated unexpectedly high concentrations of drug with a long terminal elimination half-life ($t_{1/2}$). This led to a modification of the UCN-01 administration schedule, in which the recommended phase II dose of UCN-01 is administered as a 72-h continuous infusion at 42.5 mg m^{-2} day^{-1} over a 3 day period. Subsequent courses are administered at 4-week intervals during a 36-h period (31). The extremely low clearance and small distribution volume of UCN-01 in humans could be partly due to the high degree of binding to hAGP. Although many drugs that associate with hAGP have K_a values of 10^5 to 10^6 M^{-1}, UCN-01 is unique in the tightness of its binding to hAGP, with K_a of 10^8 M^{-1}. As a consequence of this extraordinary high binding affinity, a low volume of distribution, which approximates the extracellular volume, and long $t_{1/2}$ is observed. In view of its altered pharmacokinetics due to its high interaction affinity with hAGP, the plasma levels of the hAGP are a potentially important factor in clinical treatment considerations.

hAGP is a glycoprotein that consists of 183 amino acid residues and five carbohydrate chains. The five highly sialylated complex-type-N-linked glycans contribute 45% of the molecular weight (32,33). As an acute phase reactant, hAGP's "basal" level is approximately 20 μmol/L, but it can vary from a 5- to a 10-fold range in response to stress, infection, or the effects of neoplasm in evocation of an inflammatory response. In addition, the levels of hAGP vary widely heterogeneous in cancer patients where the composition of hAGP is heterogeneous according to the type of disease, consisting of different isoforms and degrees of glycosylation. Differences in the binding of drugs to the two main genetic variants of hAGP have also been reported (25). Thus, the distribution of UCN-01 on the hAGP isoforms may also be difficult to predict.

Previous studies indicated that hAGP has one common drug binding site, which appears to be wide and flexible (34). In general, studies in our laboratory have shown that electrostatic and hydrophobic interactions are important driving forces for the binding of ligands to hAGP (35). In a study using fluorescence and ultracentrifugation experimental methods, the binding site of UCN-01 on hAGP was concluded to partly overlap with the binding site for basic drugs, acidic drugs, as well as steroid hormones (18). In order to

Table III. Binding Percentage of UCN-01 to Native and Chemically Modified hAGP at pH 7.4

	Chemically modified hAGP				
	Native	His	Lys	Trp	Tyr
Binding percentage (%)	96.33 ± 1.26	70.44 ± 2.68*	75.97 ± 1.56*	56.97 ± 2.06*	73.70 ± 1.01*

The concentrations are: [UCN-01] = [hAGP] = [chemically modified hAGP] = 20 μM.
All values are mean ± SD (n = 3).
* Statistically significant compared with native hAGP; $p < 0.01$.

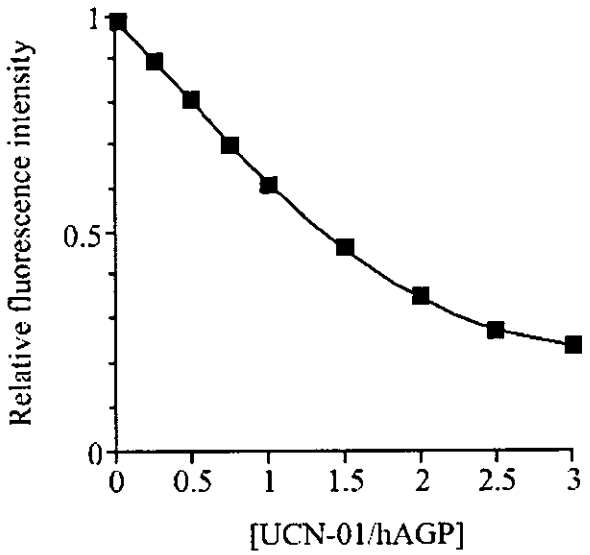

Fig. 6. Fluorescence quenching titration curve of UCN-01 binding to hAGP at pH 7.4 Concentration is: [hAGP] = 1 μM. [UCN-01] = 0 to 3 μM.

examine the ligand-binding site structural relationship of UCN-01 interactions with hAGP, the binding affinity of UCN-01, staurosporine, the "lead" compound among PKC inhibitors and UCN-02, a UCN-01 stereoisomer and weak PKC inhibitor were measured (Fig. 1). The decrease in the binding affinity followed the sequence of UCN-01 > Staurosporine > UCN-02 (Table I). It is obvious that the substituent at the C-7 position of the staurosporine molecule governs the binding affinity of UCN-01 analogues to hAGP. Interestingly, a hundred fold difference in binding affinity was recorded between UCN-01 and UCN-02, suggesting strict stereoisomeric or steric binding requirements of the UCN-01 binding site on hAGP. Meanwhile, the importance of the moiety at the C-7 position has also been reported for binding to target proteins (36,37). In a recent study, the crystal structures of staurosporine and UCN-01 in a complex with the kinase domain of PDK1 showed that, although staurosporine and UCN-01 interact with the PDK1 active site in an overall similar manner, the UCN-01 7-hydroxy group, which is not present in staurosporine, generates direct and water-mediated hydrogen bonds with active-site residues (36). On the other hand, hydrophobic interactions and hydrogen-bonding interactions were observed in the crystal structures between UCN-01 and the Chk1 kinase domain. The selectivity of UCN-01 toward Chk1 over cyclin-dependent kinases is due to the presence of a hydroxyl group in the lactam moiety, that interacts with the ATP-binding pocket. The high structural complementarity of these interactions is consistent with the potency and selectivity of UCN-01 (37). The interaction of the substituent at the C-7 position of UCN-01 to its binding protein is very important in terms of the selectivity of pharmacological activity and binding affinity, as is also the case of its binding to hAGP. It is, thus, apparent that the 7-hydroxy group of UCN-01 may play a key role in abnormally strong binding for hAGP.

The binding interactions of a series of basic ligands with hAGP were reported to increase with increasing pH. It was proposed that hydrophobic interactions dominate the high-affinity binding to hAGP (28). Meanwhile, Taheri *et al.* proposed a binding site for local anesthetics on F1*S of hAGP that is largely comprised of a structurally accommodating hydrophobic pocket, perhaps with the ability to form hydrogen bond to H-donor and -acceptor groups on the ligand and with a basic residue, mostly charged at neutral pH, that is located close to the aromatic group on bound drug molecules (38). In the present binding study, the binding of UCN-01 to hAGP also increased with increasing pH and the maximum binding of UCN-01 to hAGP was observed at pH 7.4 (96.33%). On the other hand, a low percentage of binding percentage was observed at pH 6 (69.74%) (Fig. 3). It is known that a tumor micro-environment is frequently more acidic by approximately 0.3–0.5 pH units, compared with that of its surrounding normal tissues. A decrease in the binding of UCN-01 in an acidic environment may partly contribute to the generation of free UCN-01 molecules for its anticancer activity at the cancer tissues.

hAGP exists in a variety of sialylated states which can be influenced by certain disease states. In a study investigating the effect of the sialylation state of hAGP on the binding of a model cationic drug, propranolol, the use of desialylated hAGP resulted in a modest increase in the propranolol free fraction (26). Since the binding percentage of UCN-01 to hAGP is more than 95%, an increase in the free fraction could be of clinical importance. Therefore, the binding of UCN-01 to native and desialylated hAGP was determined by ultracentrifugation. The percentage binding of desialylated hAGP was found to be comparable to that of native hAGP, suggesting that the influence of sialylation on UCN-01 binding is negligible. While asialoglycoprotein including desialylated hAGP is commonly known to be internalised by hepatocytes via receptor-mediated endocytosis, staurosporine has been reported to be an effective inhibitor of a liver uptake mechanism such as this (39). Since the liver is the major organ for the metabolism of desialylated hAGP, the significance of such protein trafficking inhibition by UCN-01 in contributing to its own low clearance deserves further investigation.

hAGP plasma concentrations differ depending on the type of cancers and such changes in the expression of the genetic variants of hAGP can be observed in various types of cancer. hAGP can be produced as three main genetic variants, the A variant and the F1 and S variants, which are encoded by two different genes (Fig. 2). Differences in the binding of ligands to hAGP variants have been reported. The ligand binding site of the F1*S variant is reported to be a relatively large hydrophobic pocket that is able to accommodate a variety of chemical structures, whereas the A variant binding site appears to be of smaller size and has a greater ligand specificity. The selective binding of disopyramide and methadone to the A variant and the preferential binding of dipyridamole to the F1*S variant mixture have been reported. On the other hand, lignocaine and chlorpromazine showed a slight preference for binding to the A variant and to the F1*S mixture, respectively. However, progesterone showed no selectivity with regard to any of the variants of hAGP (13). In the present study, no significant difference was detected for the binding of UCN-01 to the F1*S and A variants of hAGP (Table II). Hence, a change in the composition of the variants of hAGP may not be of clinical significance, despite the significant species difference in UCN-01 binding, in which a subsequent administration of hAGP to rats that had been infused

with UCN-01 actually caused a redistribution of the drug back to the blood stream from the peripheral tissues (40).

Chemical modification of His, Lys, Trp and Tyr residues of hAGP caused a marked decrease in the binding of UCN-01 (Table III). The binding percentage of UCN-01 to Trp-modified hAGP was also the lowest among all of the modified samples (Table III). Furthermore, modification of Trp residues also caused a marked decrease in the binding of staurosporine (data not shown). It is obvious that Trp residues are important in maintaining the tertiary structure of hAGP which is necessary for the high affinity binding of UCN-01. In addition, results of binding to chemically modified hAGP suggested that at least one Trp residue is involved in the binding of UCN-01 to hAGP. The involvement of Trp residues in UCN-01 binding could also be observed in the tryptophanyl fluorescence spectra where increasing UCN-01 concentrations led to a decrease in the fluorescence intensity of Trp residues of hAGP (Fig. 6). Interestingly, all three Trp residues are conserved in both F1*S and A variants of hAGP (Fig. 2) which showed no binding discrimination for UCN-01 (Table II).

Although we managed to identify the key factors for the unusually high binding affinity between UCN-01 and hAGP, namely the substituent at C-7 of the UCN-01 molecule and the Trp residues of hAGP, evidence is still lacking for suggesting a direct interaction between these two major factors. Among the three Trp residues of hAGP, two are relatively shielded from the bulk solvent, while the third Trp residue is located on the periphery of the domain (41). Trp^{25} has been deduced to be located deep in the binding pocket while Trp^{122} in the central hydrophobic pocket of the protein (42). Therefore, Trp^{160} could be the one that is exposed to the bulk solvent. Quantification of the chemical modification in the present study showed that, on average, about one Trp residue per mole of hAGP was modified. Since the modification of Trp residues was carried out under mild conditions without a surfactant present, the possibility of Trp^{160} being the modified residue is high. This suggests that Trp^{160} is the Trp residue that is involved in the binding of UCN-01. The identification of the specific Trp residue of hAGP involved in the high affinity binding of UCN-01 is currently underway in our laboratory. UCN-01 represents an initial candidate for a differentially selective protein kinase inhibitor. The results of this study will help in the informed design of future second generation approaches, as well as to serve as basis for further exploration of the potential of staurosporine pharmacophores which could lead to opportunities for structure-based optimization of PDK1 inhibitors.

ACKNOWLEDGMENTS

We wish to thank Kyowa Hakko Kogyo Co. (Shizuoka, Japan) for providing us UCN-01, UCN-02 and staurosporine to carry out the experiments in this study.

REFERENCES

1. S. Akinaga, K. Gomi, M. Morimoto, T. Tamaoki, and M. Okabe. Antitumor activity of UCN-01, a selective inhibitor of protein kinase C, in murine and human tumor models. *Cancer Res.* **51**: 4888–4892 (1991).
2. S. Akinaga, K. Nomura, K. Gomi, and M. Okabe. Effect of UCN-01, a selective inhibitor of protein kinase C, on the cell-cycle distribution of human epidermoid carcinoma, A431 cells. *Cancer Chemother. Pharmacol.* **33**:273–280 (1994).
3. C. M. Seynaeve, M. Stetler-Stevenson, S. Sebers, G. Kaur, E. A. Sausville, and P. J. Worland. Cell cycle arrest and growth inhibition by the protein kinase antagonist UCN-01 in human breast carcinoma cells. *Cancer Res.* **53**:2081–2086 (1993).
4. A. M. Senderowicz. Small-molecule cyclin-dependent kinase modulators. *Oncogene* **22**:6609–6620 (2003).
5. E. Fuse, H. Tanii, N. Kurata, H. Kobayashi, Y. Shimada, T. Tamura, Y. Sasaki, Y. Tanigawara, R. D. Lush, D. Headlee, W. D. Figg, S. G. Arbuck, A. M. Senderowicz, E. A. Sausville, S. Akinaga, T. Kuwabara, and S. Kobayashi. Unpredicted clinical pharmacology of UCN-01 caused by specific binding to human alpha1-acid glycoprotein. *Cancer Res.* **58**:3248–3253 (1998).
6. Z. H. Israili and P. G. Dayton. Human alpha-1-glycoprotein and its interactions with drugs. *Drug Metab. Rev.* **33**:161–235 (2001).
7. E. Fuse, A. Hashimoto, N. Sato, H. Tanii, T. Kuwabara, S. Kobayashi, and Y. Sugiyama. Physiological modeling of altered pharmacokinetics of a novel anticancer drug, UCN-01 (7-hydroxystaurosporine), caused by slow dissociation of UCN-01 from human alpha1-acid glycoprotein. *Pharm. Res.* **17**:553–564 (2000).
8. K. Schmid. In F.W. Putman (ed.), *The Plasma Proteins, Structure, Function and Genetic Control 1*, Academic Press, New York, 1975 pp. 183–288.
9. I. Yuasa, S. Weidinger, K. Umetsu, K. Suenaga, G. Ishimoto, B. C. Eap, J. C. Duche, and P. Baumann. Orosomucoid system: 17 additional orosomucoid variants and proposal for a new nomenclature. *Vox Sang.* **64**:47–55 (1993).
10. L. Dente, G. Ciliberto, and R. Cortese. Structure of the human alpha 1-acid glycoprotein gene: sequence homology with other human acute phase protein genes. *Nuc. Acids Res.* **13**:3941–3952 (1985).
11. L. Dente, M. G. Pizza, A. Metspalu, and R. Cortese. Structure and expression of the genes coding for human alpha 1-acid glycoprotein. *EMBO J.* **6**:2289–2296 (1987).
12. C. M. Merritt and P.G. Board. Structure and characterisation of a duplicated human alpha 1 acid glycoprotein gene. *Gene* **66**:97–106 (1988).
13. F. Herve, G. Caron, J. C. Duche, P. Gaillard, N. Abd Rahman, A. Tsantili-Kakoulidou, P. A. Carrupt, P. d'Athis, J. P. Tillement, and B. Testa. Ligand specificity of the genetic variants of human alpha1-acid glycoprotein: generation of a three-dimensional quantitative structure-activity relationship model for drug binding to the A variant. *Mol. Pharmacol.* **54**:129–138 (1998).
14. J. W. Holladay, M. J. Dewey, B. B. Michniak, H. Wiltshire, D. L. Halberg, P. Weigl, Z. Liang, K. Halifax, W. E. Lindup, and D. J. Back. Elevated alpha-1-acid glycoprotein reduces the volume of distribution and systemic clearance of saquinavir. *Drug Metab. Dispos.* **29**:299–303 (2001).
15. C. Gambacorti-Passerini, M. Zucchetti, D. Russo, R. Frapolli, M. Verga, S. Bungaro, L. Tornaghi, F. Rossi, P. Pioltelli, E. Pogliani, D. Alberti, G. Corneo, and M. D'Incalci. Alpha 1 acid glycoprotein binds to imatinib (STI571) and substantially alters its pharmacokinetics in chronic myeloid leukemia patients. *Clin. Cancer Res.* **9**:625–632 (2003).
16. J. C. Duche, S. Urien, N. Simon, E. Malaurie, and I. Monnet. and J. Barre. Expression of the genetic variants of human alpha-1-acid glycoprotein in cancer. *Clin. Biochem.* **33**:197–202 (2000).
17. P. A. Bombardt, J. E. Brewer, and M. G. Johnson. Protein binding of tirilazad (U-74006) in human, Sprague-Dawley rat, beagle dog and cynomolgus monkey serum. *J. Pharmacol. Exp. Ther.* **269**:145–150 (1994).
18. N. Kurata, S. Matsushita, K. Nishi, H. Watanabe, S. Kobayashi, A. Suenaga, and M. Otagiri. Characterization of a binding site of UCN-01, a novel anticancer drug on alpha-acid glycoprotein. *Biol. Pharm. Bull.* **23**:893–895 (2000).
19. K. Yamaoka, Y. Tanigawara, T Nakagawa, and T. Uno. A pharmacokinetic analysis program (multi) for microcomputer. *J. Pharmacobiodyn.* **4**:879–885 (1981).
20. K. J. Fehske, W. E. Muller, and U. Wollert. The modification of the lone tryptophan residue in human serum albumin by 2-hydroxy-5-nitrobenzyl bromide. Characterization of the modified protein and the binding of L-tryptophan and benzodiazepines to

the tryptophan-modified albumin. *Hoppe Seylers Z. Physiol. Chem.* **359**:709–717 (1978).
21. M. Sokolovsky, J. F. Riordan, and B. L. Vallee. Tetranitromethane. A reagent for the nitration of tyrosyl residues in proteins. *Biochemistry* **5**:3582–3589 (1966).
22. H. Fraenkel-Conrat. Methods for Investigating the Essential Groups for Enzyme Activity. *Methods Enzymol.* **4**:247–269 (1957).
23. R. Haynes, D. T. Osuga, and R. E. Feeney. Modification of amino groups in inhibitors of proteolytic enzymes. *Biochemistry* **6**:541–547 (1967).
24. J. L. Roosemont. Reaction of histidine residues in proteins with diethylpyrocarbonate: differential molar absorptivities and reactivities. *Anal. Biochem.* **88**:314–320 (1978).
25. F. Herve, E. Gomas, J. C. Duche, and J. P. Tillement. Evidence for differences in the binding of drugs to the two main genetic variants of human alpha 1-acid glycoprotein. *Br. J. Clin. Pharmacol.* **36**:241–249 (1993).
26. S. Primozic and P. J. McNamara. Effect of the sialylation state of alpha 1-acid glycoprotein on propranolol binding. *J. Pharm. Sci.* **74**:473–475 (1985).
27. I. Takahashi, Y. Saitoh, M. Yoshida, H. Sano, H. Nakano, M. Morimoto, and T. Tamaoki. UCN-01 and UCN-02, new selective inhibitors of protein kinase C. II. Purification, physico-chemical properties, structural determination and biological activities. *J. Antibiot. (Tokyo)* **42**:571–576 (1989).
28. S. Urien, F. Bree, B. Testa, and J. P. Tillement. pH-dependence of warfarin binding to alpha 1-acid glycoprotein (orosomucoid). *Biochem. J.* **289**:767–770 (1993).
29. K. Schmid, R. B. Nimerg, A. Kimura, H. Yamaguchi, and J. P. Binette. The carbohydrate units of human plasma alpha1-acid glycoprotein. *Biochim. Biophys. Acta* **492**:291–302 (1977).
30. M. H. Rahman, T. Miyoshi, K. Sukimoto, A. Takadate, and M. Otagiri. Interaction mode of dicumarol and its derivatives with human serum albumin, alpha 1-acid glycoprotein and asialo alpha 1-acid glycoprotein. *J. Pharmacobiodyn.* **15**:7–16 (1992).
31. E. A. Sausville, S. G. Arbuck, R. Messmann, D. Headlee, K. S. Bauer, R. M. Lush, A. Murgo, W. D. Figg, T. Lahusen, S. Jaken, X. Jing, M. Roberge, E. Fuse, T. Kuwabara, and A. M. Senderowicz. Phase I trial of 72-hour continuous infusion UCN-01 in patients with refractory neoplasms. *J. Clin. Oncol.* **19**:2319–2333 (2001).
32. J. M. Kremer, J. Wilting, and L. H. Janssen. Drug binding to human alpha-1-acid glycoprotein in health and disease. *Pharmacol. Rev.* **40**:1–47 (1988).
33. M. J. Treuheit, C. E. Costello, and H. B. Halsall. Analysis of the five glycosylation sites of human alpha 1-acid glycoprotein. *Biochem. J.* **283**:105–112 (1992).
34. T. Miyoshi, R. Yamamichi, T. Maruyama, A. Takadate, and M. Otagiri. Further characterization of reversal of signs of induced cotton effects of dicumarol derivatives-alpha 1-acid glycoprotein systems by protriptyline. *Biochem. Pharmacol.* **43**:2161–2167 (1992).
35. T. Miyoshi, R. Yamamichi, T. Maruyama, and M. Otagiri. Reversal of signs of induced cotton effects of dicumarol-alpha 1-acid glycoprotein systems by phenothiazine neuroleptics through ternary complexation. *Pharm. Res.* **9**:845–849 (1992).
36. D. Komander, G. S. Kular, J. Bain, M. Elliott, D. R. Alessi, and D. M. Van Aalten. Structural basis for UCN-01 (7-hydroxystaurosporine) specificity and PDK1 (3-phosphoinositide-dependent protein kinase-1) inhibition. *Biochem. J.* **375**:255–262 (2003).
37. B. Zhao, M. J. Bower, P. J. McDevitt, H. Zhao, S. T. Davis, K. O. Johanson, S. M. Green, N. O. Concha, and B. B. Zhou. Structural basis for Chk1 inhibition by UCN-01. *J. Biol. Chem.* **277**:46609–46615 (2002).
38. S. Taheri, L. P. Cogswell, A. Gent, and G. R. Strichartz. Hydrophobic and ionic factors in the binding of local anesthetics to the major variant of human alpha1-acid glycoprotein. *J. Pharmacol. Exp. Ther.* **304**:71–80 (2003).
39. R. J. Fallon and M. Danaher. The effect of staurosporine, a protein kinase inhibitor, on asialoglycoprotein receptor endocytosis. *Exp. Cell Res.* **203**:420–426 (1992).
40. N. Kurata. Pharmacokinetics and pharmacodynamics of a novel anti-cancer drug, indrocarbazole analogue, UCN-01. Ph.D. Thesis, Kumamoto University, Japan (2000).
41. M. L. Friedman, K. T. Schlueter, T. L. Kirley, and H. B. Halsall. Fluorescence quenching of human orosomucoid. Accessibility to drugs and small quenching agents. *Biochem. J.* **232**:863–867 (1985).
42. T. Kute and U. Westphal. Steroid-protein interactions. XXXIV. Chemical modification of alpha1-acid glycoprotein for characterization of the progesterone binding site. *Biochim. Biophys. Acta* **420**:195–213 (1976).

Drug Metab. Pharmacokin. 19 (4): 297-302 (2004).

Regular Article

Kinetic Studies of Covalent Binding between N-acetyl-L-cysteine and Human Serum Albumin Through a Mixed-disulfide Using an N-methylpyridinium Polymer-based Column

Daisuke HARADA[1], Makoto ANRAKU[2], Hikaru FUKUDA[2], Shinsaku NAITO[1], Kumiko HARADA[2], Ayaka SUENAGA[2] and Masaki OTAGIRI[2]

[1]*Division of Pharmacology, Drug Safety and Metabolism, Otsuka Pharmaceutical Factory, Inc., Tokushima, Japan*
[2]*Graduate School of Pharmaceutical Sciences, Kumamoto University, Kumamoto, Japan*

Full text of this paper is available at http://www.jssx.org

Summary: The binding properties of the disulfide covalent bond between N-acetyl-L-cysteine (NAC) and human serum albumin (HSA) were investigated. HSA, purified from either healthy subjects or renal failure patients, was incubated with NAC in buffer and analyzed by 4VP-EG-Me column chromatography, which can distinguish between the redox states of the only free thiol of HSA. Although intact HSA was found to consist of mainly three sub-types, marcaptoalbumin (HMA), cysteine-bound nonmercaptoalbumin (HNA_{Cys}) and a further oxidized form (HNA_{oxy}), the formation of a new type of nonmercaptoalbumin (HNA_{NAC}) was confirmed after incubation with NAC. Interestingly, NAC rapidly dissociated Cys from HNA_{Cys} and NAC itself bound very slowly to HSA. These findings suggest that the interaction between NAC and HSA proceeds in a 2-step processes. The first-order binding and dissociation rate constants of NAC to healthy HSA ($k_{on,NAC}$) and Cys from healthy HNA_{Cys} ($k_{off,Cys}$) were approximately 0.0032 and 1.3 (h^{-1}), respectively. On the other hand, HSA from renal failure patients showed decreased HMA and increased HNA_{Cys}. The $k_{on,NAC}$ and $k_{off,Cys}$ were 0.0094 and 0.45 (h^{-1}), respectively, suggesting that the pathological state may affect the binding properties of HSA and NAC.

Key words: human serum albumin; N-acetyl-L-cysteine; covalent binding; disulfide bond; kinetics

Introduction

Human serum albumin (HSA) contains a free thiol that can interact outside of the albumin molecule and is derived from a cysteine residue at the 34th amino acid (Cys^{34}).[1] HSA can bind various thiol-containing compounds *via* a mixed-disulfide bond, which forms between the free thiol of Cys^{34} and a thiol from the other compound. Studies using various thiol-containing drugs have shown that the formation and degradation of such covalent bonds proceeds not instantaneously but time-dependently and that the covalent-binding ratio between the thiol-containing drug and albumin varies with time.[2-5] Therefore, elucidation of the properties of such protein-drug binding over time is an important pharmacokinetic issue in order to understand the efficacy of thiol-containing drugs.

We previously reported the kinetic profiles of covalent binding between albumin and N-acetyl-L-cysteine (NAC), which is a thiol-containing drug used as a mucolytic agent, by determining the free- and protein-bound drug concentrations.[4,5] On the other hand, Narazaki *et al.* have reported kinetic and mechanical profiles of the binding between HSA and other thiol-containing drugs, such as Captopril and Bucillamine, by directly detecting the conformational changes of the Cys^{34} moiety of albumin using *N*-methylpyridinium polymer-based (4VP-EG-Me) column chromatography.[2,3]

In the present study, we directly quantified HSA using a 4VP-EG-Me column after incubation with NAC and analyzed the kinetic properties of covalent protein binding in order to obtain basic information on the covalent binding between HSA and NAC. In addition, we investigated the effect of pathological conditions on binding kinetics of NAC using HSA purified from the

Received; May 22, 2004, Accepted; June 25, 2004
To whom correspondence should be addressed: Daisuke HARADA, *Division of Pharmacology, Drug Safety and Metabolism, Otsuka Pharmaceutical Factory, Inc., 115 Aza kuguhara, Tateiwa, Muya-cho, Naruto, Tokushima 772-8601, Japan. Tel. +81-88-685-1151, Fax. +81-88-686-8176, E-mail: haradada@otsukakj.co.jp*

renal failure patients as well as the healthy subjects because the covalent protein-binding formation between HSA and thiol-containing drug, Bucillamine, increased in several pathological states, such as renal failure, diabetes, hepatitis, and rheumatism.[6]

Methods

Materials: HSA was purchased from Chemo-Sero-Therapeutic Research Institute (Kumamoto, Japan) or purified from human serum. Purification of albumin from human serum was performed according to the method of Watanabe *et al.*[7] Briefly, serum was applied to a Blue Sepharose affinity chromatography column, which was pre-treated with 0.2 M sodium acetate (pH 5.5). The column was then washed with 0.2 M sodium acetate (pH 5.5) and 1 N sodium chloride, and albumin was eluted with 0.02 M sodium acetate and 3 M sodium chloride (pH 6.5). The albumin containing fraction was dialyzed against water, freeze-dried, and de-fatted. Purification of albumin was confirmed by SDS-PAGE and Western blotting.

NAC was purchased from Sigma Chemical Co. (St. Louis, MO, USA). N-acetyl-L-[1-^{14}C] cysteine (^{14}C-NAC) was synthesized by Amersham Pharmacia Biotech Ltd. (Buckinghamshire, UK) and was purified before use. The radiochemical purity was >95% and the specific radioactivity was 2.15 MBq/μmol NAC. All other chemicals or solvents were of analytical or HPLC grade.

Human serum: The protocol used in this study followed the tenets of the Declaration of Helsinki promulgated in 1964 and was approved by the institutional review board and informed consent was obtained from all subjects. Five stable hemodialysis patients (3 men and 2 women) aged 71 to 77 years, of dialysis age ranging from 5 to 9 years, were enrolled in the study. Five gender-matched healthy subjects were also investigated as a control group. End-stage renal failure was the result of glomerulonephritis (n = 5).

HPLC conditions: The HPLC system comprised an LC-4A pump (Shimadzu, Tokyo, Japan) equipped with a gradient programmer and a Shimadzu SPD-2AS ultraviolet (UV) monitor. The column packing material, *N*-methylpyridinium polymer cross-linked with ethylene glycol dimethacrylate (4VP-EG-Me), was prepared as described previously.[8] HSA was eluted using a 30-min linear gradient of 0 to 0.5 M sodium chloride in 0.05 M Tris-AcOH buffer (pH 6.5) at a flow rate of 0.5 mL/min at 25°C and the detection wavelength was 280 nm.

Definition of HSA: HSA can be classified into two main sub-types; mercaptoalbumin and nonmercaptoalbumin (**Fig. 1**). These sub-types are referred to as HMA and HNA, respectively. Although HNA is a general term that includes both the L-cysteine (Cys)-bound type and the oxidized type, HSA-Cys disulfide and oxidized

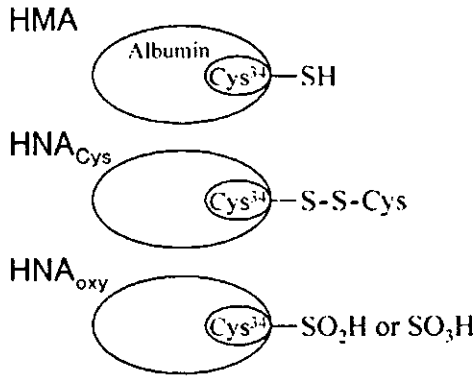

Fig. 1. Illustrations showing intrinsic HSA sub-types classified by the structure of the Cys^{34} moiety. HMA: human mercaptoalbumin. HNA: human nonmercaptoalbumin.

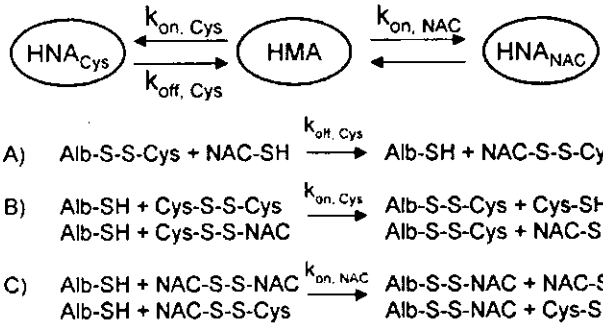

Fig. 2. Diagram showing the conversion of HSA among its sub-types through a thiol-disulfide exchange reaction when NAC is added and its kinetic model.

HSA are referred to as HNA_{Cys} and HNA_{oxy}, respectively in this study (**Fig. 1**).

Assay conditions: HSA was dissolved in phosphate buffer (pH 7.4, 0.067 M, $\mu = 0.15$) from which endogenous oxygen had previously been removed by sonication and nitrogen replacement. The HSA solution (approximately 300 μM) was preincubated at 37°C for 5 min and then approximately 1500 μM NAC was added. The mixture was incubated at 37°C under anaerobic conditions. Aliquots were analyzed by HPLC at various incubation times.

For analysis of HSA incubated with ^{14}C-labelled NAC, column eluent was collected at 30-second intervals and the radioactivity of each fraction were determined.

Calculation of kinetic parameters: The reaction between HSA and low-molecular thiol-compounds was expected to proceed through the thiol-disulfide exchange reaction. Possible mechanisms of the interactions between HSA, NAC, and Cys, which is the most abundant thiol-compound retained by HSA, are shown in **Fig. 2**. The kinetic parameters $k_{off,Cys}$, $k_{on,Cys}$, and $k_{on,NAC}$ were defined as the apparent first-order rate constants, representing the dissociation of Cys from HNA_{Cys}, the

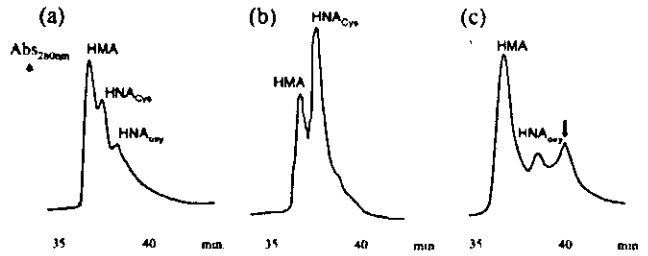

Fig. 3. UV chromatogram of HSA after application to the 4VP-EG-Me column. (a) HSA from healthy volunteer. (b) HSA from renal failure patient. (c) HSA from healthy volunteer incubated with NAC at 37°C for 48 h. Assay conditions are described in the Materials and Methods section.

binding of Cys to HMA, and the binding of NAC to HMA, respectively. These parameters were obtained as follows.

The concentrations of each sub-type of HSA were indicated as a percentage of each chromatographic peak against the total HSA peak area. The common logarithms of the concentrations were plotted against the incubation time and then correlation lines were obtained by the least-squares method. The slopes of these lines correspond to the rate constants (h^{-1}) for the reactions.

Results

HPLC chromatogram of HSA: HSA was primarily separated into three sub-types (in order of abundance; HMA, HNA_{Cys}, and HNA_{oxy}) on the 4VP-EG-Me column chromatography (**Fig. 3**). The ratio of three sub-types ($HMA:HNA_{Cys}:HNA_{oxy}$) in HSA from healthy subjects was approximately 5:4:1 (**Fig. 3(a)**). On the other hand, HSA from renal failure subjects showed an extreme decrease in HMA and an increase in HNA_{Cys} (**Fig. 3(b)**).

Following incubation of HSA with NAC at 37°C, the HNA_{Cys} peak was almost disappeared and a new peak was formed behind the HNA_{oxy} peak (**Fig. 3(c)**). When incubated with ^{14}C-labelled NAC, the radioactive peak corresponded to the newly formed peak (**Fig. 4**), thus suggesting that the newly formed peak corresponded to the stable complex of HSA and NAC, i.e., HSA-NAC mixed disulfide (HNA_{NAC}).

Time-courses of each HSA sub-type after incubation with NAC: **Figure 5** shows the time-concentration plots of each albumin sub-type (HMA, HNA_{Cys}, HNA_{oxy}, and HNA_{NAC}) after incubation of healthy HSA with NAC. During the 2 hours from the start of incubation, HNA_{Cys} rapidly decreased and HMA increased in a complementary manner, and this was followed by a slow reversal, with HNA_{Cys} and HMA increasing and decreasing, respectively. These changes suggest that HNA_{Cys} was rapidly divided into HMA and free Cys by NAC during the first stage of incubation, and Cys then

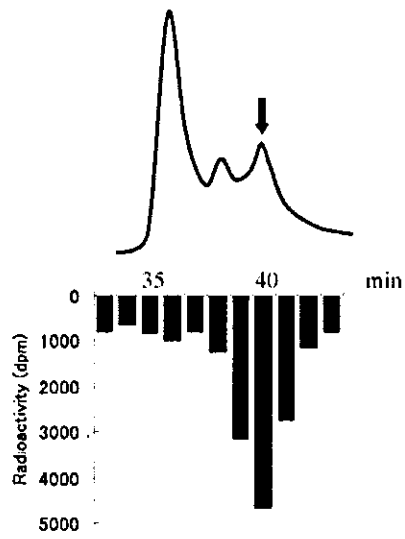

Fig. 4. UV chromatogram and radioactivity distribution of column eluent fractions after HSA was incubated with ^{14}C-labelled NAC for 48 h.

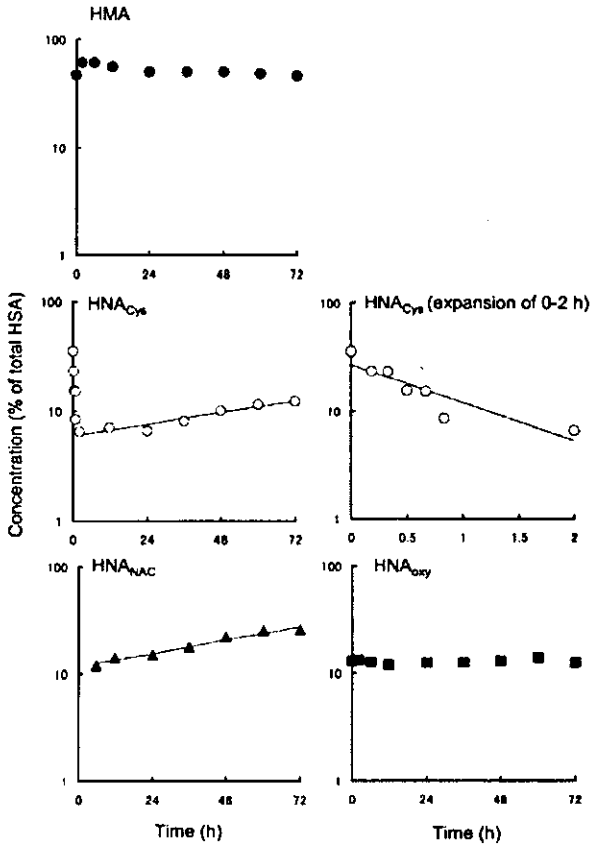

Fig. 5. Time-concentration plots of HSA sub-types after incubation with NAC. Concentrations are indicated as the percentage of each sub-type against the total HSA detected as chromatographic peak area. In the case of HNA_{Cys}, the short time range (0 ~ 2 h) was expanded as a separate figure. Each solid line indicates the correlation obtained by the least-squares method.